

Feasibility of Single-Step EDC Coupling for Immobilisation of Xylanase on Biobased Microspheres

Maria Beatriz Catalão e Oliveira de Graça Ferrão

Thesis to obtain the Master of Science Degree in

Chemical Engineering

Supervisor(s): Prof. Dr. Pedro Fardim
Prof. Dr. Eduardo Jorge Morilla Filipe

Examination Committee

Chairperson: Prof. Dr. António Maçanita
Supervisor: Prof. Dr. Pedro Fardim
Member of the Committee: Prof. Dr. Pedro Fernandes

June 2017

Acknowledgments

First of all, I would like to take my promotor at KU Leuven, Prof. Dr. Pedro Fardim, for providing me with this opportunity, for his guidance, scientific advice and help throughout this work and final revision. To my promotor at IST, Prof. Dr. Eduardo Filipe, who supported my idea of going abroad and helped in all the necessary steps. To Prof. Dr. Kristel Bernaerts, who allowed me to use the lab facilities at her care to perform my thesis research.

I would also like to express my sincere gratitude to Mr. Kenneth Simoens, who taught me everything I needed to know regarding the experimental work, and specially, for his never-ceasing help and patience. To Mrs. Trivedi Poonam, for taking hours of her work to give her scientific advice and even conduct an essential experiment to this work. To Mrs. Christine Wouters, for all her help and shared knowledge on the FTIR spectroscopy.

A big hug to my friends, far or close, who have accompanied me in this journey of my life, and with whom I could always count on their support. A special thanks to Carine, Luc and Astrid for making me feel at home, for being my second family, and for all the help and support throughout these past months.

I would like to thank my mom, for her dedication, love and care. For always being by my side, no matter what. Not a million words are enough to express my appreciation to my boyfriend, Simon, who reviewed all this text in long (and probably boring) phone calls, put aside his work to give me his advices/remarks, supported and believed in me, from beginning to end. Without him, this work would not be the same.

Last, but certainly not least, I would like to dedicate this work to my grandmother, who always cared deeply about my studies. Obrigada, avó, por olhares por mim. Um dia, encontrar-nos-emos novamente.

Resumo

A xilanase é uma enzima hidrolítica largamente utilizada em aplicações industriais. Tem surgido um crescente interesse pela imobilização desta enzima uma vez que permite a sua consecutiva reutilização, reduz a contaminação das proteínas pela enzima, torna fácil a separação do producto, entre outras vantagens.

Dando continuidade a estudos prévios, este trabalho tem como principal objectivo estudar a praticabilidade de imobilizar xilanase em microesferas feitas de material biológico renovável, mais precisamente esferas de celulose, um polissacarídeo abundante na natureza, e, por conseguinte, com um impacto ambiental muito reduzido.

Inicialmente, foi realizada uma oxidação TEMPO (N-oxil-2,2,6,6-tetrametilpiperidina) com o objectivo de produzir grupos carboxilo (-COOH) na superfície dos esferas de celulose. De seguida, a quantidade dos grupos carboxilo foi medida através de uma titulação conductométrica. Ulteriormente, foi levada a cabo a imobilização da xilanase nos esferas de celulose usando o método *single-step EDC (hidroclorato de 1-etil-3-(3-dimetilaminopropil) carbodiimida) coupling*. Para retirar conclusões, a actividade catalítica da enzima livre foi comparada com a actividade catalítica da enzima imobilizada.

Os resultados demonstram que a oxidação foi bem sucedida. Contudo, a imobilização não foi totalmente alcançada, como comprovado pela diferença entre os valores da actividade catalítica da enzima livre (13.4 ± 3.77 U.mg⁻¹ xilanase) e da enzima imobilizada nas 4 amostras de esferas de celulose (0.513 ± 0.254 , 0.528 ± 0.246 , 0.867 ± 0.083 , 0.761 ± 0.176 U.mg⁻¹ xilanase), sendo expectável uma maior similitude. A causa mais plausível para este desfecho é o facto de se ter utilizado apenas o reagente EDC, que provocou a reticulação da xilanase, visto que contém grupos carboxilo e grupos amina na sua composição.

Esta descoberta confirma que o método *single-step EDC coupling* não está totalmente optimizado para a xilanase (e, possivelmente para outras enzimas que contenham grupos carboxilo e grupos amina). Assim, futuras investigações devem apurar métodos mais adequados para a imobilização da xilanase (tal como o método *two-step EDC/sulfo-NHS coupling*).

Palavras-chave: xilanase, enzima, imobilização, esferas de celulose, oxidação, método *single-step EDC coupling*.

Abstract

Xylanase is a hydrolytic enzyme, that is widely used in industrial applications. A great interest for the immobilisation of this enzyme has arisen, since it allows the consecutive reutilisation of the enzyme, reduction of product contamination by the enzyme, easy separation from the product, and other advantages.

Building further on previous studies, this work aims to investigate the feasibility of immobilisation of xylanase enzymes on biobased microspheres, more precisely beads made out of cellulose, which is a polysaccharide abundant in nature, and thus has a very low environmental footprint.

Firstly, a TEMPO (2,2,6,6-tetramethyl-piperidin-1-yl)oxyl oxidation reaction was performed with the goal of producing carboxyl groups (-COOH), on the cellulose beads. Afterwards, the quantity of carboxyl groups was measured through a conductometric titration. Subsequently, immobilisation of xylanase on the cellulose beads was carried out by the single-step EDC (1-ethyl-3-(3-dimethylaminopropyl)carbodiimide hydrochloride) coupling method. To draw conclusions, the catalytic activity of the free enzyme was compared with the catalytic activity of the immobilised enzyme.

The results of the oxidation experiment show that it was successful. However, the immobilisation was not completely achieved, as proven by the difference between the catalytic activities of the free enzyme ($13.4 \pm 3.77 \text{ U}\cdot\text{mg}^{-1}$ xylanase) and the immobilised enzyme on the 4 samples of cellulose beads (0.513 ± 0.254 , 0.528 ± 0.246 , 0.867 ± 0.083 , $0.761 \pm 0.176 \text{ U}\cdot\text{mg}^{-1}$ xylanase), which were expected to be similar. The most plausible cause for these results was the use of solely EDC, which led to the cross-linking of the amino and carboxyl groups of xylanase.

This discovery acknowledges that the single-step EDC coupling method is not fully optimised for xylanase (and, perhaps, for other enzymes that have both amino and carboxyl groups). Hence, future research should investigate more suited methods for the immobilisation of xylanase (such as the two-step EDC/Sulfo-NHS coupling method).

Keywords: Xylanase, enzyme, immobilisation, cellulose beads, oxidation, single-step EDC coupling method.

Contents

Acknowledgments	iii
Resumo	v
Abstract	vii
List of Tables	xiii
List of Figures	xv
Nomenclature	xvii
Glossary	xix
1 Introduction	1
2 State of the art	3
2.1 Polysaccharides	3
2.1.1 Cellulose	3
2.1.2 Xylan	4
2.2 Cellulose microspheres	7
2.2.1 Preparation	7
2.2.2 Characterisation	9
2.2.3 Functionalisation	9
2.2.3.1 TEMPO oxidation	10
2.2.4 Applications	11
2.3 Enzymes	11
2.3.1 Xylanases	14
2.3.1.1 Enzymatic mechanism	16
2.3.1.2 Fungal xylanases	18
2.4 Immobilisation of enzymes	18
2.4.1 Single-step EDC coupling method	21
3 Experimental	23
3.1 TEMPO oxidation of cellulose beads	23
3.1.1 Material	23
3.1.2 Equipment	24
3.1.3 Method	24

3.2	Fourier Transform Infrared Spectroscopy	25
3.2.1	Materials	25
3.2.2	Equipment	25
3.2.3	Method	25
3.3	Conductometric titration	26
3.3.1	Materials	26
3.3.2	Equipment	26
3.3.3	Method	26
3.4	Single-step EDC coupling	27
3.4.1	Materials	27
3.4.2	Equipment	28
3.4.3	Method	28
3.5	Bradford protein assay	29
3.5.1	Materials	29
3.5.2	Equipment	30
3.5.3	Method	30
3.6	Assay of endo-1-4- β -xylanase activity	30
3.6.1	Material	30
3.6.2	Equipment	30
3.6.3	Method	31
4	Results and Discussion	35
4.1	TEMPO oxidation of cellulose beads	35
4.1.1	Qualitative results	35
4.1.2	Quantitative results	37
4.2	Bradford protein assay	41
4.3	Enzyme activity	42
4.3.1	Comparison between the catalytic activity of the free enzyme with the immobilised enzyme	42
4.3.2	Occurrence of side reactions	43
4.3.3	Study to determine the occurrence of cross-linking	45
4.3.4	Analysis of the time-frame on the single-step EDC coupling	46
4.3.5	Mass-transfer effects	48
5	Conclusions	49
5.1	Future Work	50
	Bibliography	53
A	Conductometric titration	57

List of Tables

3.1	Amount of reagents used for the TEMPO oxidation (mmol.g ⁻¹ cellulose beads).	25
3.2	Quantity of EDC (g) required for xylanase immobilisation assuming the same quantity of COOH groups as reported in [34].	29
4.1	Comparison of the pH values reported in the literature [26] with the ones obtained in this study.	36
4.2	Amount of COOH groups (mmol.g ⁻¹) determined by equation 3.1. The mass of dried beads (g), volume of NaOH (ml) and the concentration of NaOH (0.01 M) were used in the equation.	40
4.3	Comparison of the quantity of carboxyl groups of the literature [34] with this research. . .	40
4.4	Amount, in mg, of xylanase present on E ₁ and the supernatant of samples 1 to 4.	41
4.5	Amount, in mg, of xylanase attached to the carboxyl groups of the cellulose beads.	41
4.6	Catalytic activity (U.mg ⁻¹ xylanase) of the free and immobilised xylanase.	42
4.7	Immobilisation yield of samples 1, 2, 3 and 4.	42
4.8	Comparison between the actual used quantities and post-hoc required quantities of EDC (g).	44
4.9	Catalytic activity (U.mg ⁻¹ xylanase) of the xylanase with EDC.	46
4.10	Catalytic activity (U.mg ⁻¹ xylanase) of the immobilised xylanase with a small modification (i.e. the EDC and the enzyme solution were added 2h apart) of the protocol.	47
B.1	Absorbance of the samples tested using the Bradford protein assay.	62

List of Figures

2.1	Chemical structure of cellulose. Where n is equal to the degree of polymerisation, while 3 refers to the number of hydroxyl groups present in each AGU unit. (Figure adapted from [11]).	4
2.2	Model structure of a plant cell highlighting the cell wall (figure taken from [16]).	5
2.3	Chemical structure of the xylan backbone and the attack sites of the enzymes that cleave xylan. Xylanases and β -Xylosidases cleave the backbone, while the side chains are cleaved by α -l-arabinofuranosidases, α -d-glucuronidases, acetyl xylan esterases, ferulic acid esterases. (Figure taken from [14]).	6
2.4	Chemical structure of Arabinoxylans (figure taken from [17]).	6
2.5	Chemical structure of Glucuronoxylans (figure taken from [17]).	7
2.6	Chemical structure of Glucuronoarabinoxylans (figure taken from [17]).	7
2.7	Cellulose dissolution techniques followed by shaping into beads (figure taken from [19]).	8
2.8	Preparation techniques to obtain cellulose beads. From left to right: dropping, <i>jet cutting</i> , <i>spinning drop atomisation</i> , <i>spinning disc atomisation</i> and dispersion (figure taken from [19]).	9
2.9	Scheme of the TEMPO oxidation of cellulose under weakly acidic or neutral conditions (figure taken from [20]).	10
2.10	The pathway of a catalysed and an uncatalysed reaction (figure taken from [22]).	12
2.11	<i>Michaelis-Menten</i> model (figure adapted from [22]).	13
2.12	The kinetic of allosteric enzymes (figure taken from [22]).	13
2.13	Differences between two different types of inhibitors (figure taken from [22]).	14
2.14	Disposition of the 6 families with endo-1-4- β -xylanase activity (figure based on [24]).	15
2.15	Representative image of the structures of the 6 families with endo-1-4- β -xylanase activity (figure taken from [25]).	16
2.16	Scheme of the inverting mechanism (a) and the retaining mechanism (b) of glycoside hydrolases (figure adapted from [27]).	17
2.17	Immobilisation methods. From left top to right bottom: covalent bonding, adsorption, cross-linking and entrapment (figure taken from [30]).	19
2.18	The different types of cross-linked enzyme aggregates, CLEAs (figure taken from [21]).	20
2.19	Chemical structure of EDC (figure taken from [31]).	21
2.20	Reaction scheme using EDC as crosslinker (figure taken from [32]).	22

3.1	Image of the cellulose beads seen through the microscope. The beads have a diameter of approximately 500 μm .	24
3.2	Water bath Julabo SW22. (figure taken from [33]).	24
3.3	S470 Mettler Toledo Seven Excellence™ pH/Conductivity meter (figure taken from [35]).	26
3.4	Conductivity ($\mu\text{S}\cdot\text{cm}^{-1}$) vs volume of NaOH (ml) (figure taken from [36]).	27
3.5	Grant Bio PTR60 360° Vertical Multi-Function Rotator (figure taken from [37]).	28
3.6	Illustration of the single-step EDC coupling method. Same procedure made for the remaining samples (i.e sample 2, 3, and 4).	29
3.7	On the left (a): termomixer F1.5; on the right (b): centrifuge 5810 R; on the bottom (c): DR 5000™ UV-Vis Spectrophotometer (figures taken from [38] [39] [40]).	31
3.8	Illustration of the assay of endo-1-4- β -xyylanase activity. The same procedure was done for the remaining samples.	32
4.1	Samples 1 to 4 (left to right) of the oxidised cellulose beads. The NaClO ₂ increases from left (i.e. sample 1) to right (i.e sample 4) of the oxidised cellulose beads.	36
4.2	Fourier Transformed Infrared Spectra of the reference and oxidised cellulose beads. A characteristic peak of the carboxyl acid salt at 1600 cm^{-1} is evident for samples 1 to 4, which is absent for the reference cellulose beads.	37
4.3	Conductometric titration graph of sample 1.	38
4.4	Zone 1 of the conductometric titration graph.	38
4.5	Zone 2 of the conductometric titration graph.	39
4.6	Zone 3 of the conductometric titration graph.	39
4.7	Possible side reactions of EDC that block the formation of the amide bond (figure adapted from [31]).	43
4.8	Scheme of the performed trial to prove the occurrence of cross-linking. EDC, in varying quantities, was mixed with enzyme solution to compare the catalytic activity of the free enzyme.	45
4.9	Scheme of the single-step EDC coupling method (figure adapted from [31]).	47
5.1	Two-step EDC/sulfo-NHS coupling method (figure taken from [31]).	51
A.1	Conductometric titration graph of sample 2.	57
A.2	Zone 2 of the conductometric titration graph of sample 2.	58
A.3	Conductometric titration graph of sample 3.	58
A.4	Zone 2 of the conductometric titration graph of sample 3.	59
A.5	Conductometric titration graph of sample 4.	59
A.6	Zone 2 of the conductometric titration graph of sample 4.	60
B.1	Scheme of the dilutions made to obtain the standard curve. All dilutions were made with distilled water.	61
B.2	Standard curve of the Bradford protein assay.	62

Nomenclature

ΔG Gibbs energy

ΔG^\ddagger Activation energy

ΔG_S^\ddagger Free energy of the substrate

$\Delta G_{X^\ddagger}^\ddagger$ Free energy of the transition state

K_M *Michaelis* constant

K_{eq} Equilibrium constant

V_o Reaction velocity

V_{max} Maximum rate

[S] Substrate concentration

Å Ångström

Da Dalton

R Universal gas constant

T Temperature

Glossary

AGU	D-anhydroglucopyranose
AX	Arabinoxylans
Araf	Arabinofuranose
CAX	Cellulose xanthate
CA	Cellulose acetate
CLEAs	Cross-linked aggregates
CLECs	Cross-linked crystals
CLEs	Cross-linked enzymes
CP	Critical Point
EDC	1-ethyl-3-(3-dimethylaminopropyl) carbodi- imide hydrochloride
FTIR	Fourier Transform Infrared
GAX	Glucuronoarabinoxylans
GX	Glucuronoxylans
GlcA	Glucuronic acid
ILs	Molten organic salts
IUPAC	International Union of Pure and Applied Chem- istry
MW	Molecular weight
MeGlcA	4-O-methyl glucuronic acid
NMR	Nuclear Magnetic Resonance
SAXS	Small angle X-ray scattering
SEM	Scanning Electron Microscopy
TEMPO	(2,2,6,6-tetramethyl-piperidin-1-yl)oxyl
XOS	Xylooligosaccharides
Xyl	1-4 linked β -D-xylopyranosyl

Chapter 1

Introduction

In this thesis, a new study of the feasibility of immobilisation of the enzyme xylanase on the cellulose beads was carried out.

Thanks to enzyme immobilisation, the difficulty of recovery and reuse of the enzymes, as well as the long-term instability were overcome. Instead, higher efficiency of catalysis, higher selectivity towards the substrates and a low impact in the environment were obtained.

Essential components to carry out an immobilisation are the enzyme, the carrier and the method. Nowadays, enzymes are used in a range of diverse products such as textiles, food, pulp and paper, pharmaceutical products, diagnostics tests, among other things [1]. In this work, xylanase, an hydrolytic enzyme that cleaves the backbone of xylan, a hemicellulose present in wood and plants, was studied. Xylanase has major applications on the food industry, where it is used to accelerate the baking process, by breaking down hemicellulose. Thus, xylanase improves dough features and increases the quality of bread and other bakery products [2]. Moreover, xylanase can be used on the pharmaceutical industry for producing xylooligosaccharides (XOS), which have health promoting properties such as treatment and prevention of gastrointestinal infections, action against skin and hair disorders, osteoporosis, otitis, among others [3].

The carrier is extremely important for the performance of the immobilised enzyme. Therefore, cellulose beads were used because they are classified as excellent carriers [4] due to their many characteristics (high surface area, porosity, stability, and reactivity).

Along the years, several methods for the immobilisation of enzymes have been developed. These are divided into 4 wide groups as listed in 1995 by the International Union of Pure and Applied Chemistry (IUPAC): 1) covalent bonding of the enzyme to a water-insoluble matrix; 2) adsorption of the enzyme to a water-insoluble matrix; 3) intermolecular cross-linking of enzyme molecules using multi-functional reagents; 4) entrapment of the enzyme into a water-insoluble matrix or a semipermeable membrane [5]. A covalent bonding method (single-step EDC coupling method) was used for the immobilisation of xylanase on the cellulose beads. The aim was to crosslink the carboxyl groups (-COOH) present on the cellulose beads with the amino groups of xylanase by using EDC (1-ethyl-3-(3-dimethylaminopropyl) carbodiimide hydrochloride) as cross-linker.

The main goal of this work was to study the effect of this immobilisation method on the catalytic activity of xylanase. Therefore, it was necessary to perform a TEMPO (2,2,6,6-tetramethyl-piperdin-1-yl)oxyl oxidation to produce carboxyl groups, on the cellulose beads. Once the results of this experiment were quantified by means of a conductometric titration, the single-step EDC coupling method was carried out. In the end, the catalytic activity was studied.

The structure of this thesis is as follows:

Chapter 2 covers the state of the art which provides the necessary background for a full understanding of the concepts and objectives of this research. Chapter 3 presents all the materials, equipment and methodology for each performed technique: TEMPO oxidation, conductometric titration, single-step EDC coupling method, assay of endo-1-4- β -xylanase activity and Bradford protein assay. Chapter 4 includes all results obtained and their discussion. Chapter 5 comprises the conclusions and ideas for a future research. The Appendix A and B provide supporting information concerning the conductometric titration and the Bradford protein assay.

Chapter 2

State of the art

This chapter starts with a brief introduction about polysaccharides, focusing on cellulose and xylan. The following section encompasses an explanation on cellulose microspheres, their preparation, characterisation, functionalisation, featuring TEMPO oxidation, and applications. Afterwards, an overview of the catalytic activity and performance of enzymes, including the studied enzyme, xylanase. At last, information about the main focus of this work is covered: definition, types and applications of enzyme immobilisation, highlighting the single- step EDC coupling method. All these topics allow the reader to grasp the main concepts and purposes of this research.

2.1 Polysaccharides

Polysaccharides are the combination of carbohydrates (or monosaccharides), normally more than ten, linked together by glycosidic bonds (i.e a covalent bond between a carbohydrate and another molecule). Polysaccharides with equal monosaccharides linked together are called homopolysaccharides, while different monosaccharides linked together are known as heteropolysaccharides.

Polysaccharides are used in a big range of applications such as emulsification, suspension, film forming, coating. Moreover, polysaccharides act as thickening and sizing agents in the textile, food, paper-making industry [6]. Additionally, they can be used to produce materials for different applications in several technical fields, since they are easily chemically modified. Some examples in the biomedical field are bone cements, replacement implants, drug delivery and tissue-engineering scaffolds [7], and the production of sorbents that are used in the adsorption process for waste water treatment [8].

Polysaccharides can be found spread across nature: in plants, micro-organisms, animals.

2.1.1 Cellulose

Cellulose is the most abundant polysaccharide in nature, consisting of linear D-anhydroglucopyranose units (AGU) units linked together by $\beta(1 \rightarrow 4)$ glycosidic bonds. Two units linked together, known as cellobiose, are twisted 180° with respect to one another, and disposed in a chair conformation 4C_1 . This polymer has two different ends: a non-reducing end and a reducing end. As can be seen in figure 2.1,

the non-reducing end is located the furthest to the left, and can not form any more glycosidic bonds, while the reducing end, which is located the furthest to the right, can continue the backbone chain as demonstrated by figure [9].

Cellulose is a tough, fibrous, water-insoluble polysaccharide and an important constituent of plants' cell walls, since it is used as a scaffold for the binding of other cell wall components. Depending on whether the cellulose is derived from wood or from cotton, the degree of polymerisation (the number of monomeric units in a polymer) varies around 10 000 and 15 000 of β -D-glucopyranose units, respectively [10].

Cellulose can be found in animals, bacteria, fungi, plants and algae.

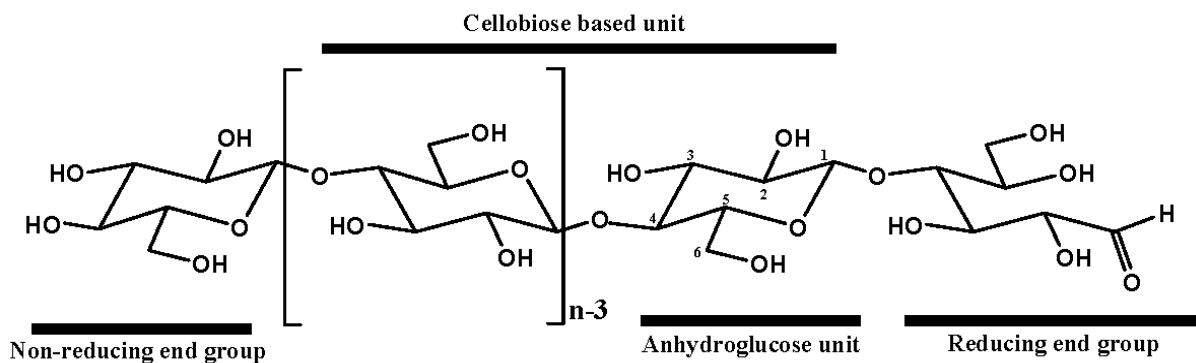


Figure 2.1: Chemical structure of cellulose. Where n is equal to the degree of polymerisation, while 3 refers to the number of hydroxyl groups present in each AGU unit. (Figure adapted from [11]).

Cellulose has been used in a multitude of applications, for more than 150 years. It is mainly known for its use in the production of paper and cardboard. At an industrial scale, it is used to produce cellulose derivatives which can be used for several ends: coatings, laminates, additives, films, pharmaceuticals, foodstuffs and cosmetics [12]. At a lab scale, bacteria (e.g. Clostridium) are able to hydrolyse cellulose to produce hydrogen [13]. These are just a few examples of applications of cellulose. It is clear that the accumulated (indirect) impact of cellulose on processes and products that permeate daily life is substantial.

2.1.2 Xylan

Xylan, the second most abundant polysaccharide, is a hemicellulose present in hardwoods (15-30 % of the cell wall content), annual plants (<30 %) and also in softwoods (7-10 %) [14]. Hardwoods are angiosperms trees, meaning that they are seed-producing flowering plants, while softwoods are gymnosperms, i.e. seed-producing non-flowering plants.

Xylan is an essential constituent of plants' cell wall. The plant cell wall is composed of 3 layers (see figure 2.2): the primary cell wall, the secondary wall and the middle lamella. The primary cell wall is formed during the cell growth and is essentially composed of polysaccharides (cellulose, pectins, hemicellulose). The secondary wall is formed after the full growth of the cell and consists of cellulose (35-50 %), xylan (20-35 %) and lignin (10-25 %). At last, the middle lamella, is the outer layer composed

of pectins. The interactions between the 3 polysaccharides present in the secondary wall protect the cellulose microfibrils and maintain the structure of the wall [15].

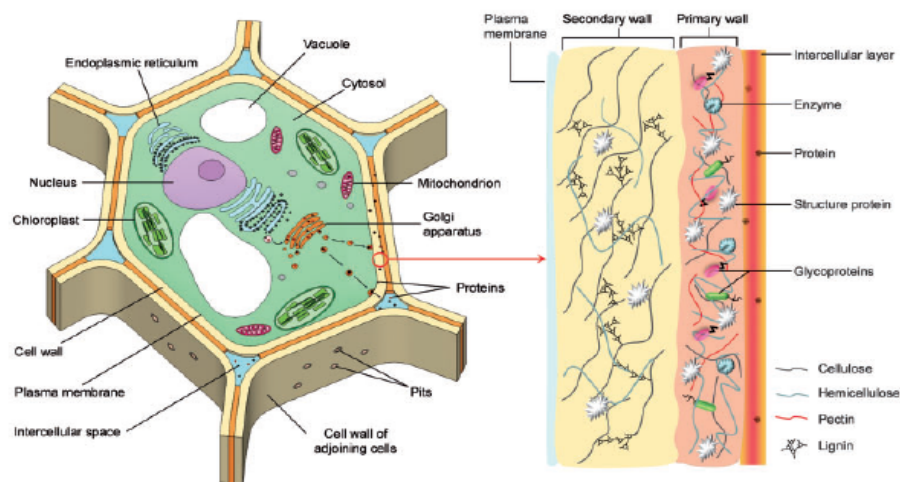


Figure 2.2: Model structure of a plant cell highlighting the cell wall (figure taken from [16]).

Xylan has a backbone composed of 1-4 linked β -D-xylopyranosyl (Xyl) units (figure 2.3). It can be replaced by glucuronic acid (GlcA) at position C2, by 4-O-methyl glucuronic acid (MeGlcA) also at position C2 and/or by arabinofuranose (Araf) at position C2 and/or C3. Several hydrolytic enzymes are required for the total breakdown of xylan due to its heterogeneity and length. The backbone is hydrolysed by xylanases, which cleave the glycosidic bonds, and D-xylosidases, which remove D-xylose from the non-reducing end. The side chains require 4 different enzymes: α -l-arabinofuranosidases, α -d-glucuronidases, acetyl xylan esterases, ferulic acid esterases. It has a degree of polymerisation between 150-200 in hardwoods, and between 70-130 in softwoods [14].

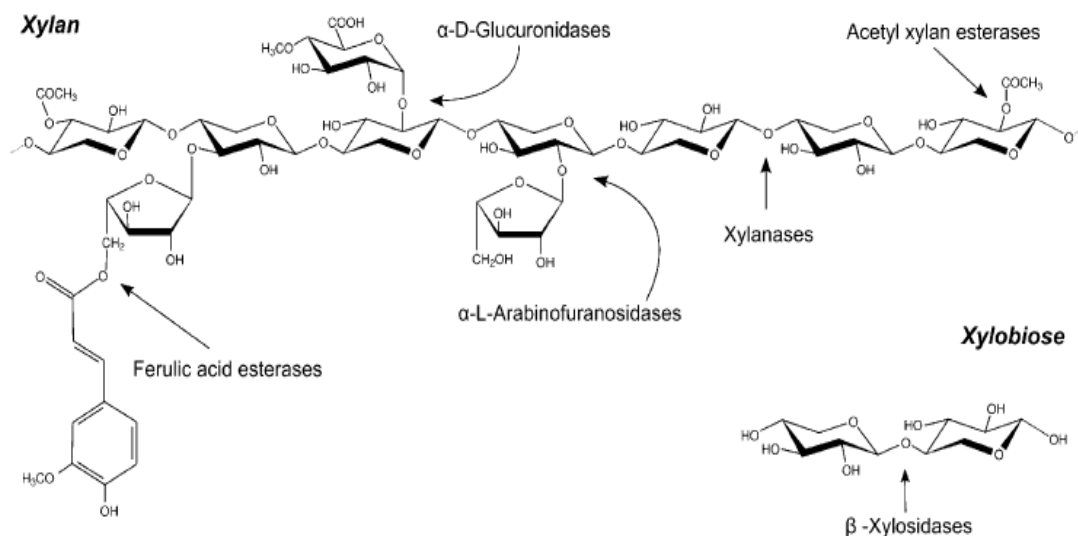


Figure 2.3: Chemical structure of the xylan backbone and the attack sites of the enzymes that cleave xylan. Xylanases and β -Xylosidases cleave the backbone, while the side chains are cleaved by α -l-arabinofuranosidases, α -d-glucuronidases, acetyl xylan esterases, ferulic acid esterases. (Figure taken from [14]).

According to which substituent is used, xylans can be divided into 3 different groups. The first group consists of Arabinoxylans (AX), as shown by figure 2.4, which have a ratio of Araf:Xyl of 1:2 or 1:1 and exist mainly in endosperm walls.

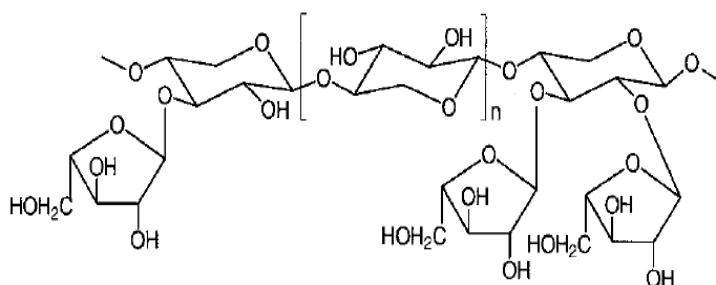


Figure 2.4: Chemical structure of Arabinoxylans (figure taken from [17]).

The second group is composed of Glucuronoxylans (GX) which have a ratio of Xyl:MeGlcA of 10:1, and are present in hardwoods (figure 2.5).

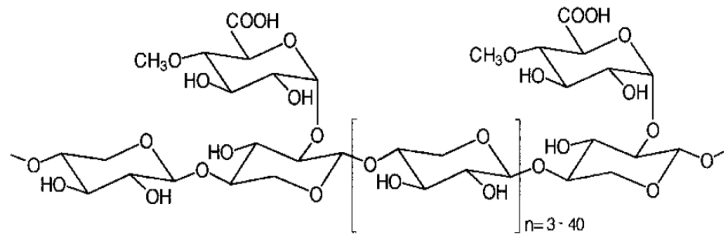


Figure 2.5: Chemical structure of Glucuronoxylans (figure taken from [17]).

The last group is comprised of Glucuronoarabinoxylans (GAX) where 3 different side chain residues, Araf, MeGlcA and GlcA, are attached to the backbone having a Xyl:Araf:GlcA ratio of 8:3:1 as demonstrated by figure 2.6. These are present in vegetative tissues of grasses, in both the primary and secondary wall .

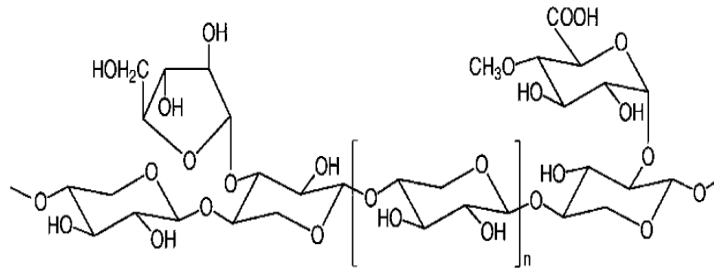


Figure 2.6: Chemical structure of Glucuronoarabinoxylans (figure taken from [17]).

It is important to take into account the choice of the side chains residues, since they regulate the reactivity of the xylan, solubility, physical conformation, and influence considerably the action of the enzymes [17].

There has been an increasing interest in employing the xylans as biodegradable polymers in several applications: coatings, encapsulation matrices, additives, and also in applications used on homopolysaccharides with high molecular weight, such as cellulose and starch. Besides this, they are able to modify the pulp fibers and to enhance the strength and bonding properties of fiber networks [18].

2.2 Cellulose microspheres

In this chapter, an overview of the preparation, characterisation, functionalisation and application of the cellulose microspheres is presented.

2.2.1 Preparation

There are three general steps to prepare cellulose beads : 1) cellulose (or derivative) dissolution, 2) shaping, 3) sol-gel transition and solidification [19]. Since cellulose is neither soluble in water or the nor

most organic compounds, several studies were conducted to circumvent this problem. Therefore, three different possibilities of dissolving cellulose are known, as shown in figure 2.7. The first method consists in using non-derivatised solvents that dissolve the cellulose through physical interactions without chemically converting its hydroxyl groups. Recent studied solvents are ILs, molten organic salts. In the second method, the cellulose is transformed into a cellulose derivative by derivatising solvents. The cellulose derivative can be shaped into cellulose beads, due to a change of pH or temperature that leads to its cleavage. The viscose process is the most used: cellulose is transformed into cellulose xanthate (CXA), a derivative soluble in NaOH, by alkalisiation, aging and CS₂ treatment, after which it can form the cellulose beads. The last method uses stable cellulose derivatives, such as cellulose acetate (CA), which unlike cellulose are soluble in the most common organic compounds. After dissolution, the cellulose derivative is shaped into beads, and shaped further on into cellulose beads.

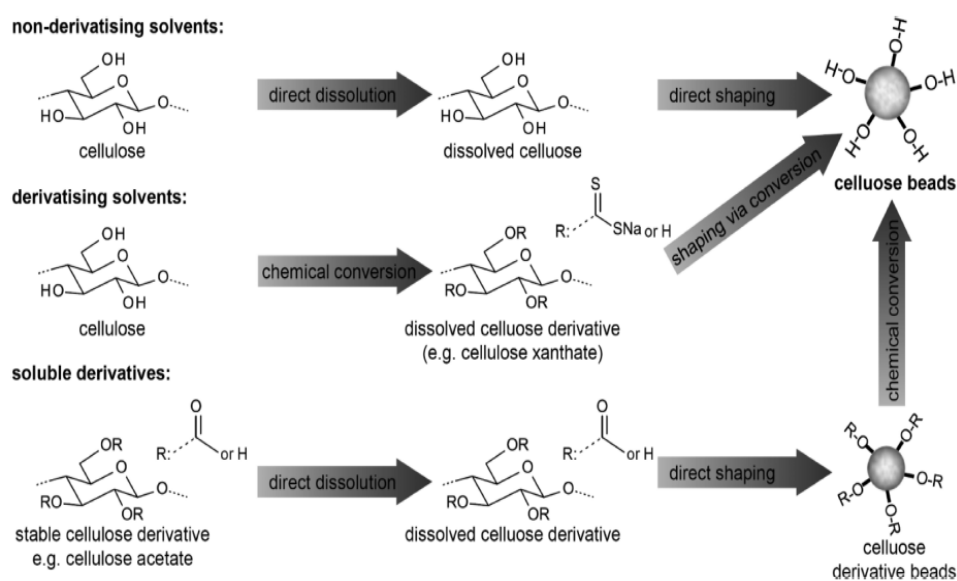


Figure 2.7: Cellulose dissolution techniques followed by shaping into beads (figure taken from [19]).

The cellulose beads can go from 3 μm up to 1-3 mm of diameter [19]. There are two possibilities to shape the beads, namely dropping or dispersion techniques. In the former technique the polysaccharide solution is forced through a thin opening, into a coagulation bath of a nonsolvent, in which they will solidify. Beads obtained by this technique have diameters between 0.5 and 3 mm. It is possible to obtain beads of different sizes and shapes by applying the same technique, but recurring to different devices. Spinning drop atomisation is a very useful technique for batch productions, which uses a rotational cylindrical vessel to produce large quantities of beads of smaller sizes (500 μm and less). Another technique used to obtain droplet beads is the spinning disc atomisation. It is also possible to obtain a constant stream instead of droplets by applying the jet cutting technique, where a rotating knife device is used.

Dispersion technique consists in forming emulsions, which contain the droplet particles, by dissolving cellulose under high rotational speed in an immiscible solvent of opposite polarity. The size of the

droplets obtained varies between 30 and 250 μm . Figure 2.8 illustrates all the techniques mentioned above.

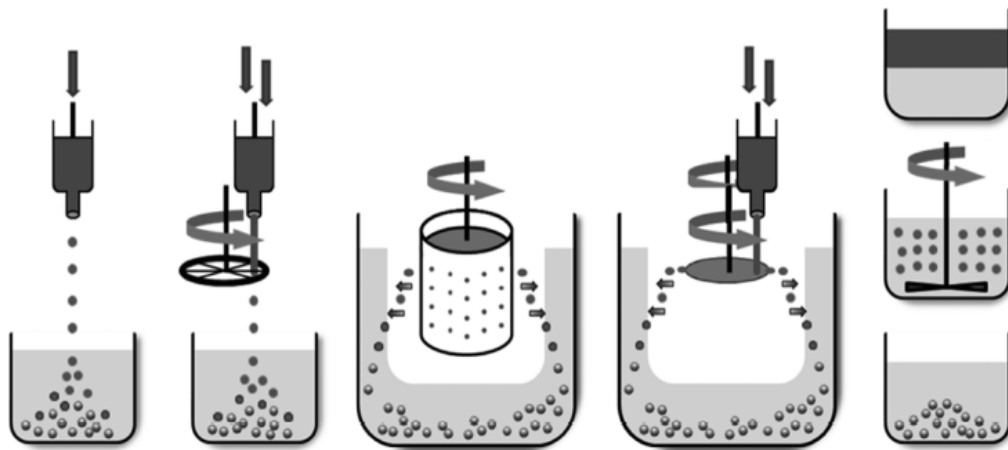


Figure 2.8: Preparation techniques to obtain cellulose beads. From left to right: dropping, *jet cutting*, *spinning drop atomisation*, *spinning disc atomisation* and dispersion (figure taken from [19]).

2.2.2 Characterisation

The size and shape of the obtained beads can be characterised by the following techniques: sieving, which is widely used in large scale productions; laser light diffraction, suited for beads obtained by dispersion techniques.

SEM (Scanning Electron Microscopy) is the most used method to measure the morphology of the beads. In order to determine the porosity and the inner surface area of the beads, it is necessary to dry them first. CP (Critical Point) drying technique was found to be the best approach to avoid damaging the beads [19]. Mercury intrusion and nitrogen sorption can also be applied after the CP drying. The former measures pores from 2 nm up to several hundreds, and the latter between 0.3 and 300 nm. The morphology of the beads can also be determined without previous drying: small angle X-ray scattering, SASX, and spin echo NMR are two techniques that use wet cellulose beads. In the case of the spin echo NMR (Nuclear Magnetic Resonance), it is only possible to obtain information concerning the porosity of the beads [19]. Mechanical stability, which constrains information regarding the maximum flow rate that can be applied in a chromatographic column, and biocompatibility, a very important aspect to measure when the cellulose beads are used for biomedical applications, are two important characteristics of the cellulose beads.

2.2.3 Functionalisation

Functionalisation allows to customise the beads, by altering their chemical structure, to a specific desired application. The most common approaches are the following: etherification, esterification, oxidation and polymer grafting. Carboxymethylation is the most applied method of etherification in the cellulose beads since it produces anionic materials, which can be used for ion exchange applications;

the formation of ethers containing sulfate groups or phosphate groups on esterification can be used in ion exchange or affinity adsorption chromatography techniques; the oxidation allows the immobilisation of enzymes to activated cellulose beads. The most known technique is the TEMPO oxidation, which is used in this work. Finally, the polymer grafting increases the length of the cellulose backbone.

2.2.3.1 TEMPO oxidation

Figure 2.9 illustrates the oxidation of the C6 primary hydroxyls of the cellulose beads to carboxylates.

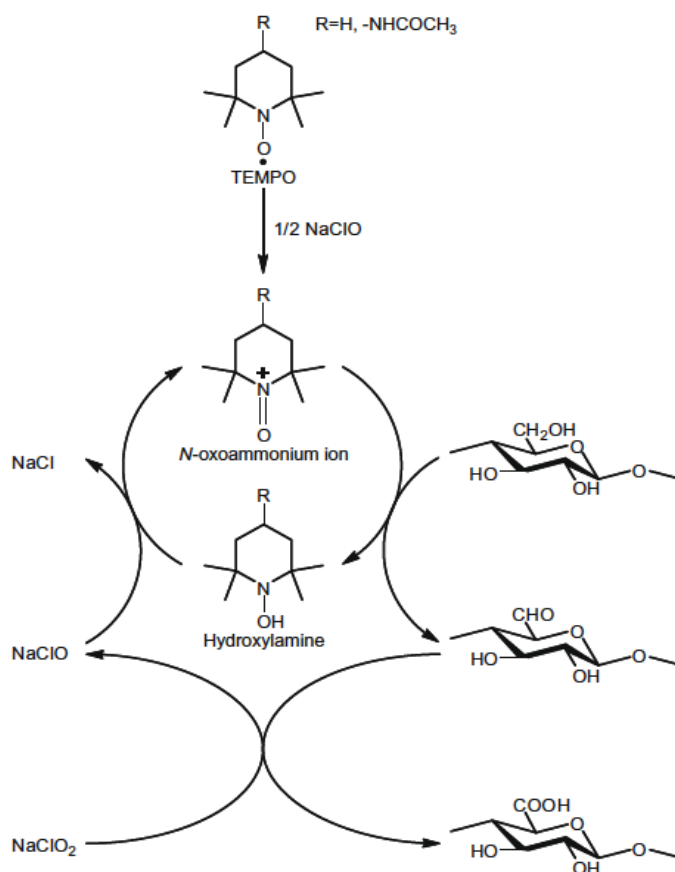


Figure 2.9: Scheme of the TEMPO oxidation of cellulose under weakly acidic or neutral conditions (figure taken from [20]) .

The system TEMPO/NaClO/NaClO₂ is used to oxidise the C6 hydroxyl groups of cellulose to carboxylates. Firstly, the TEMPO is oxidised to N-oxoammonium ion by NaClO . The N-oxoammonium ion will oxidise the hydroxyl group of the cellulose to aldehyde forming hydroxylamine. The NaClO₂ oxidises the aldehyde to carboxyl forming NaClO, which in turn oxidises the hydroxylamine back to N-oxoammonium ion.

2.2.4 Applications

Cellulose beads are widely applied in chromatography. Their shape, and the fact that they are easy to handle make them the perfect filling for chromatographic columns. Moreover, it is also possible to use cellulose beads as absorbents of dangerous metals (e.g. lead, mercury, iron, cadmium) that put in risk not only human life, but also flora and fauna, by performing cationic exchange. Therefore, modified cellulose beads with carboxyl groups, sulfonate groups, phosphate groups are applied in waste water treatment and metal ion exchange processes [19]. Protein immobilisation is a commonly used technique since the beads possess the ideal characteristics (i.e. chemical modification, sustainability and biocompatibility) to ensure a good coupling with the enzymes. Additionally, the shape of the beads guarantees a large surface area for the immobilisation.

2.3 Enzymes

Enzymes are biological catalysts. They are biocompatible, biodegradable and are derived from renewable resources [21].

To understand how enzymes operate, it is important to grasp two important thermodynamic properties: the free-energy difference also called Gibbs energy (ΔG), and the necessary energy to start a reaction. The value of ΔG does not depend on the path of the reaction, and does not provide any information about the rate of the reaction. It can be calculated using the following equation:

$$\Delta G = G_{\text{products}} - G_{\text{reactants}} \quad (2.1)$$

In case the Gibbs energy is negative ($\Delta G < 0$) it means that the reaction can occur spontaneously and no energy input is required (exergonic reaction). If the Gibbs energy is positive ($\Delta G > 0$), then the reaction is not spontaneous, and an energy input is essential to start the reaction (endergonic reaction). When there is no net change on the concentration of reactants and products, a reaction is at equilibrium ($\Delta G = 0$).

It is also possible to use another equation to obtain the value of ΔG :

$$\Delta G = \Delta G^0 + RT \ln \frac{[\text{products}]}{[\text{reagents}]} \quad (2.2)$$

where ΔG^0 is the standard free-energy change in KJ.mol^{-1} , R is the gas constant in $\text{KJ.mol}^{-1}.\text{K}^{-1}$, T is the temperature in Kelvin and $[\text{reagents}]$, $[\text{products}]$ are the concentration of the reagents and products in mol.l^{-1} , respectively.

The standard free-energy change can be related with the equilibrium constant K_{eq} of the reaction by the following equation 2.3:

$$K_{eq} = 10^{-\Delta G^0 / 2.303RT} \quad (2.3)$$

The acceleration of the reactions is related with the pathway. While transforming the reactants into

products there is a transition state in between presenting the highest free energy in the reaction progress, as can be seen in figure 2.10. Enzymes are responsible for assisting the formation of the transition state by reducing the activation energy, ΔG^\ddagger , making it possible for more molecules to reach the transition state. The activation energy is calculated by the difference between the free energy of the transition state and the free energy of the substrate (equation 2.4).

$$\Delta G^\ddagger = \Delta G^\ddagger_{X^\ddagger} - \Delta G^\ddagger_S \quad (2.4)$$

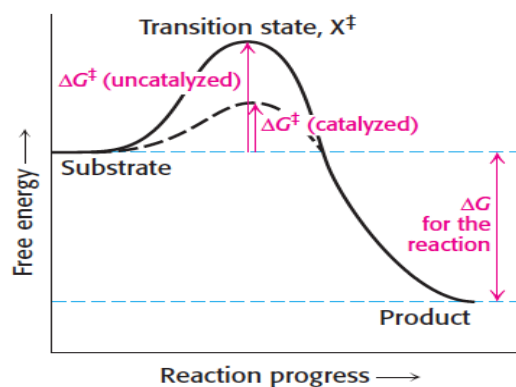


Figure 2.10: The pathway of a catalysed and an uncatalysed reaction (figure taken from [22]).

In order to have enzymatic catalysis there must first be a binding of the enzyme, E, with the substrate, S, forming ES complexes, with a consequent energy release, designated *binding energy*. The substrate binds to the enzyme by attaching itself to the active site, where the cofactor, if present, can also be attached. Enzymes can bind to substrates that have the specific shape of the active site, designated as *lock-and-key model*; or the enzyme can itself adapt to the shape of the substrate whilst binding, entitled *induced-fit model*.

The kinetics of several enzymes are given by the *Michaelis-Menten* equation, which relates the velocity of the reaction V_o with the concentration of the substrate, [S]. *Michaelis-Menten* equation is given by the following formula:

$$V_o = V_{max} \frac{[S]}{[S] + K_M} \quad (2.5)$$

in which V_{max} represents the velocity when the enzyme is saturated with substrate and K_M indicates the concentration of substrate that corresponds to half the maxim velocity rate, $\frac{V_{max}}{2}$.

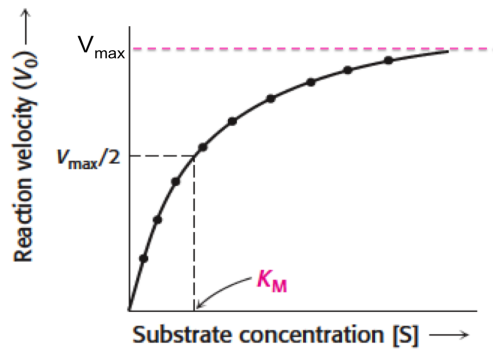


Figure 2.11: *Michaelis-Menten* model (figure adapted from [22]).

It is possible to verify, looking at figure 2.11, that if the substrate concentration [S] is much lower than K_M then the *Michaelis-Menten* equation can be well approximated by $V_o = V_{max} \frac{[S]}{K_M}$, meaning that the velocity rate is proportional to the substrate concentration, representing a first order reaction. If the substrate concentration is much higher than K_M , $V_o \simeq V_{max}$ then the reaction is of zero order, independent of the substrate concentration.

The enzymes that do not follow *Michaelis-Menten* kinetics are called allosteric enzymes. These enzymes present a sigmoidal behaviour, due to the fact that they have several subunits and active sites. They are cooperative enzymes, which means that the binding of one substrate to an active site promotes the binding of other substrates to the other active sites.

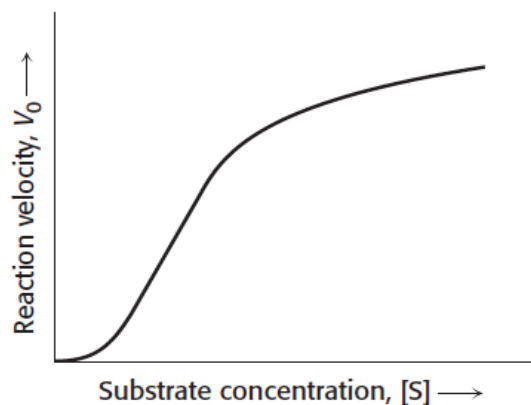


Figure 2.12: The kinetic of allosteric enzymes (figure taken from [22]).

Figure 2.12 shows that the binding of the substrates to one active site will increase the tendency of other substrates to bind to the remaining unoccupied active sites.

Enzymes can be inhibited in the presence of certain molecules or ions. The two main inhibitor types are competitive and uncompetitive inhibitors. A competitive inhibitor competes with the substrate for the same active site, while an uncompetitive inhibitor binds to a different active site than the substrate,

only when the [ES] complex is formed. Both inhibitors are responsible for reducing the rate of catalysis, although in different ways: the former leads to a decrease on the number of enzymes that bind to the substrate i.e. the value of K_M increases, while V_{max} remains the same; the latter decreases the turnover number i.e. V_{max} decreases, as well as K_M .

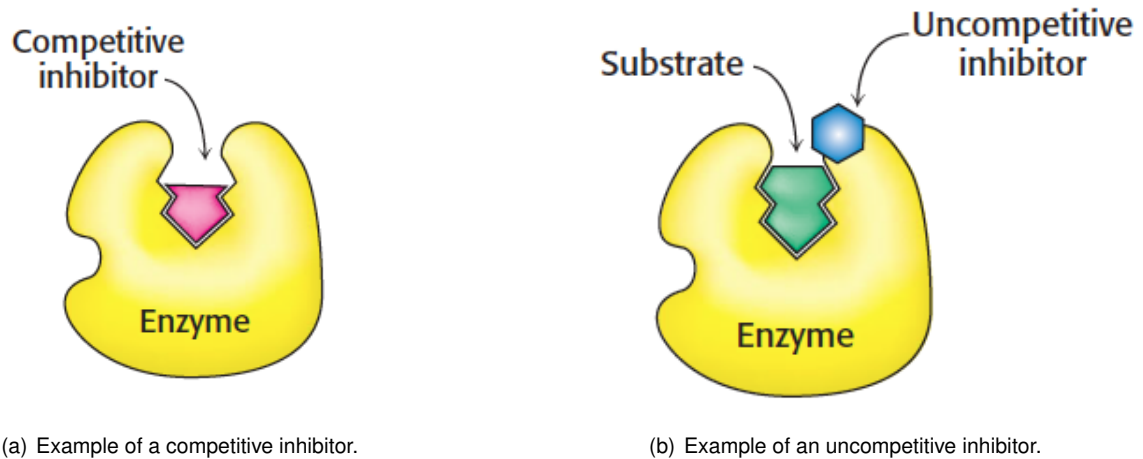


Figure 2.13: Differences between two different types of inhibitors (figure taken from [22]).

2.3.1 Xylanases

Xylanases, also known as endo-1-4- β -D-xylanases (EC 3.2.1.8), are hydrolytic enzymes that cleave the xylan backbone into small oligomers. Xylanases can either be produced by procaryotes and eucaryotes. The major producers are yeast, bacteria and fungi. This lead to a big range of types of xylanases, with more complex and distinct physical and/or chemical properties, as well as to a more efficient performance of the hydrolysis process. Because of the heterogeneity of the xylanases, a classification system was developed. The first classification system, which was implemented by Wong et al. [23], was based on the molecular weight and pI (i.e the pH at which an enzyme is not electrically charged), of the enzymes. Enzymes with molecular weight higher than 30 kDa and acidic pI form one group, while enzymes with molecular weight smaller than 30 kDa and basic pI form another. Nevertheless, some enzymes did not fit in any of these two groups, so this theory fell apart. Later on, an improved classification that separates the enzymes into different families (1-96), according to their catalytic domains and sequences, and into clans (GHA- GHN), depending on there 3D structure. From these 96 families, only 6 families show endo-1-4- β -xylanase activity: 5,7,8,10, 11 and 43 (Figure 2.14).

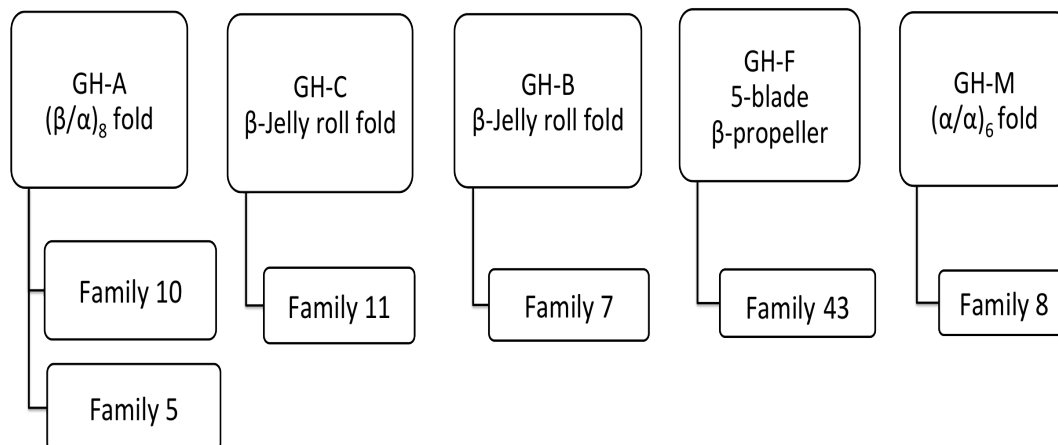


Figure 2.14: Disposition of the 6 families with endo-1-4- β -xylanase activity (figure based on [24]).

Family 5 is the largest of the 96 families, with 467 sequences, and only seven amino acid residues. Cellulase, licheninase, β -mannosidase, also belong to this family. Despite the fact that endo-1-4- β -xylanases belong to family 8, the main enzymes present are cellulases. The enzymes included in family 10 usually have a high MW and low pI, while in family 11 enzymes have a low MW and high pI. The former is composed of endo-1-4- β -xylanases, endo-1-3- β -xylanases (EC 3.2.1.32) and cellobiohydrolases, the latter is only composed of xylanases. Regarding family 7 and 43, little information is known, since only one enzyme has been found in each family [25] (figure 2.15).

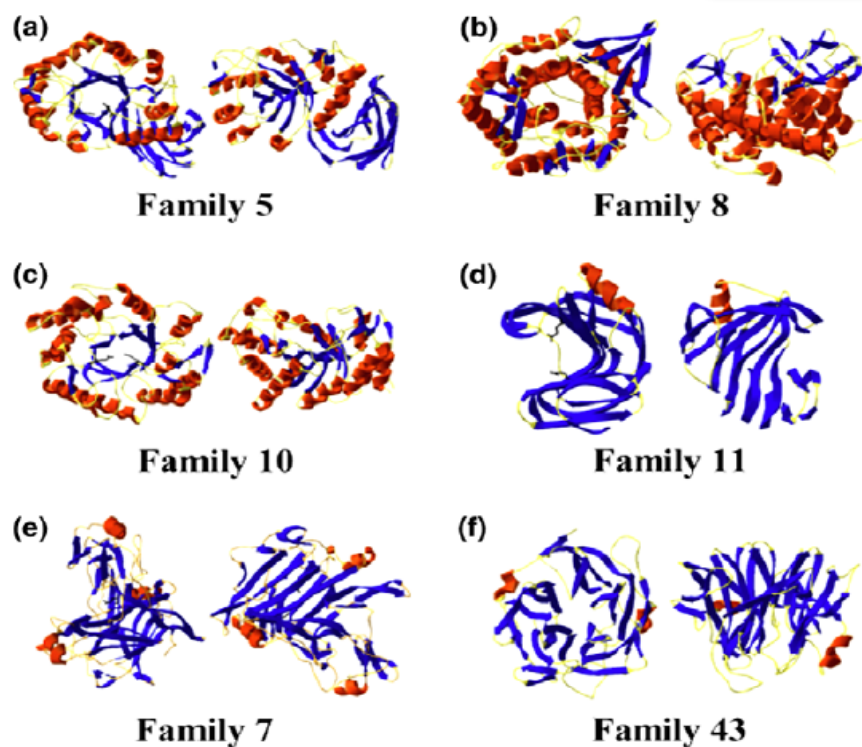


Figure 2.15: Representative image of the structures of the 6 families with endo-1-4- β -xylanase activity (figure taken from [25]).

Xylanases, nowadays, have several applications. In the paper industry, enzymes are used in the bleaching process. In the food-industry, the hemicellulose present on the wheat-flour is hydrolysed by the xylanases contributing to a softer and easier to mold dough. Moreover, xylanases can also be used on the manufacturing of biscuits since it improves its uniformity, texture and palability. In the animal feed industry, xylanases are used to break down non-nutricional hemicelluloses (arabinoxylans). The food industry also benefits from the use of xylanases, mainly for improving the yield using liquefaction, increasing the stability of the pulp and the quantity of aromas recovered and reducing the viscosity [26]. On the pharmaceutical industry, xylanases are used to produce xylooligossacharides (XOS), which have health promoting properties such as the treatment and prevention of gastrointestinal infections, action against skin and hair disorders, osteoperosis, otitis, among others [3].

The xylanase used in this work, which culture is unknown, was compared with *Aspergillus niger*, a fungus, for being the most common of the genus *Aspergillus*.

2.3.1.1 Enzymatic mechanism

As explained in section 2.1.2, the break down of xylan's backbone requires several enzymes. Glycoside hydrolases are a large group of hydrolytic enzymes, which are responsible for the cleavage of the glycosidic bonds. Xylanase, the enzyme under study here, belongs to this group. The hydrolysis of the glycosidic bond of a polymer (in this case xylan which is represented by the acetal in figure 2.16) requires two amino acids (i.e. residues present on the active site of the enzyme, that intervene in the

breaking down of bonds). For endo-1-4- β -D-xylanases, the intervening amino acids are glutamic acids, which each have two carboxyl groups (-COOH) and one amino group (-NH₂) [24]. The carboxyl groups are the intervening groups in the hydrolysis process. The enzymatic hydrolysis can have one of the two stereochemical outcomes: retention or inversion of anomeric configuration. Therefore, two distinct methods are presented in figure 2.16.

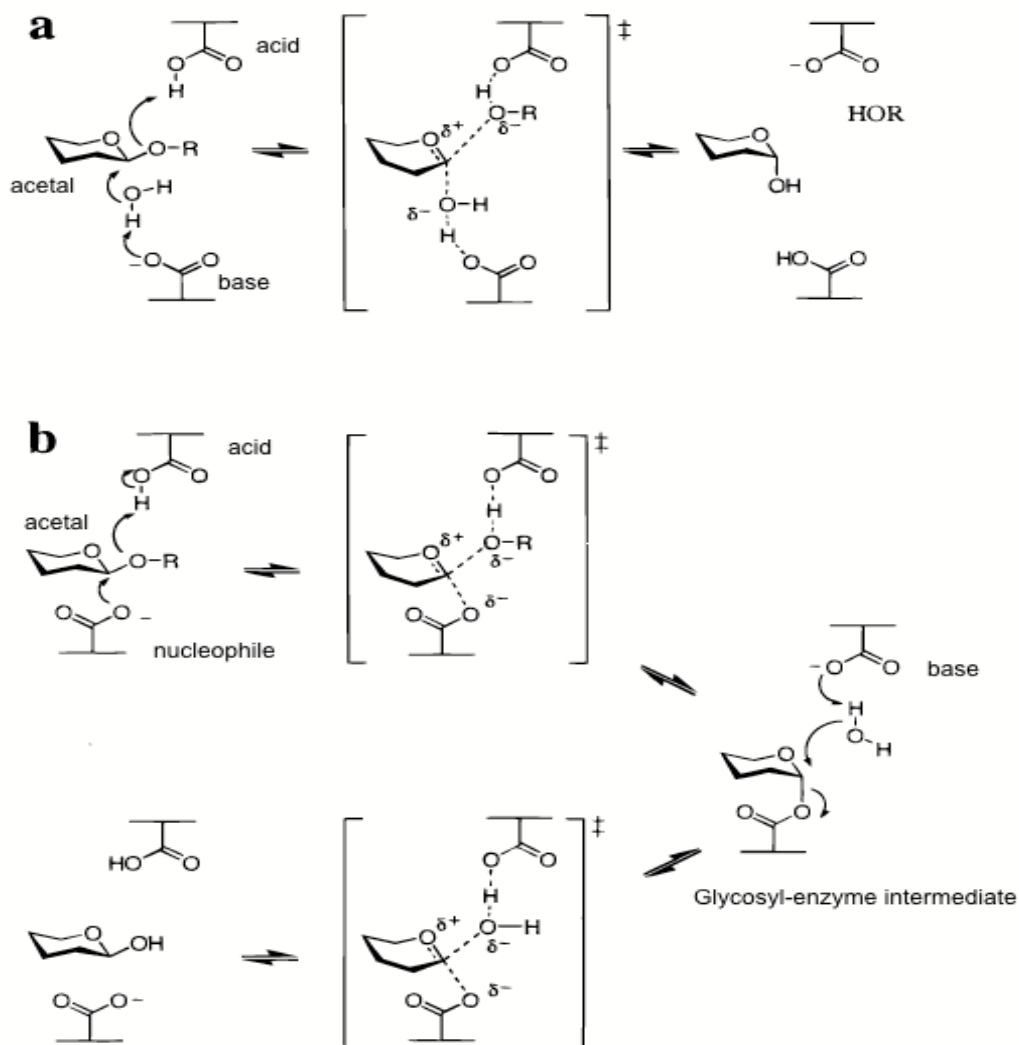


Figure 2.16: Scheme of the inverting mechanism (a) and the retaining mechanism (b) of glycoside hydrolases (figure adapted from [27]).

The inverting mechanism shown in figure 2.16 (a) uses a direct displacement mechanism requiring an oxocarbenium ion-like transition state (i.e. a positive charge is placed on the oxygen atom). The carboxyl group in the proximity of the anomeric carbon (i.e. the carbon at which anomers rotate) acts as a base, while the other carboxyl group, of the same enzyme, acts as an acid. They are placed approximately 10.5 Å apart, allowing the binding of the water molecule with the carboxyl groups and the anomeric carbon. On the other hand, the retaining mechanism shown in figure 2.16 (b) uses a double-displacement which leads to the formation of a glycosyl-enzyme intermediate. In the first step, the (acid) carboxyl group protonates the glycoside oxygen, while the (nucleophile) carboxyl group forms the inter-

mediate. In the second step, the (acid) carboxyl group behaves as a base and desprotonises the water molecule that attacks the anomeric carbon. The distance between the two residues is approximately 5.5 Å [27]. Xylanase uses the retaining mechanism to hydrolyse the glycosidic bonds of xylan [24].

2.3.1.2 Fungal xylanases

Aspergillus niger and *Trichoderma longibrachiatum*, which grow in mesophilic conditions, are the most commonly used fungi in the production of xylanases. However, studies on extremophilic fungi have also been carried out since they produce enzymes with higher stability [26].

One of the big advantages of working with fungi is the fact that they produce and expel the xylanases into the medium without bursting a cell. Besides, fungi produce higher quantities of xylanases compared with bacteria [28].

2.4 Immobilisation of enzymes

The immobilisation of enzymes is a relatively low-cost and simple operation that allows the continuous and repetitive use of the enzymes, in which a stable and active biocatalyst is obtained. This technique is of great interest for its efficiency, selectivity and for its environmentally friendly catalysis. The use of an enzyme in an immobilised form brings several advantages: it is easier to handle the enzyme, leads to a straightforward separation of the enzyme and the product, the possibility exists of re-using the enzyme and minimises the contamination of the product [21].

Every immobilised enzyme is characterised by non-catalytic and catalytic parameters. The former refers to the physical and chemical properties such as size, shape, length; the latter concerns the activity, stability and selectivity, and all catalytic functions. The non-catalytic properties of an enzyme are taken into account, so that they fit with the type of reactor, the process conditions, the reaction medium and the reaction. Preferably enzymes with catalytic parameters that lead to high productivity, few or none side reactions, longer durability of the catalyst are chosen. The goal is to choose the parameters that will lead to an easy separation of the immobilised enzyme from the reaction mixture, an accessible control of the process and a widely applicable and recyclable immobilised enzyme [29].

Along the years, several methods for the immobilisation of enzymes have been developed. These are divided into 4 wide groups as listed in 1995 by the International Union of Pure and Applied Chemistry (IUPAC): 1) covalent bonding of the enzyme to a water-insoluble matrix; 2) adsorption of the enzyme to a water-insoluble matrix; 3) intermolecular cross-linking of enzyme molecules using multi-functional reagents; 4) entrapment of the enzyme into a water-insoluble matrix or a semipermeable membrane [5] (figure 2.17).

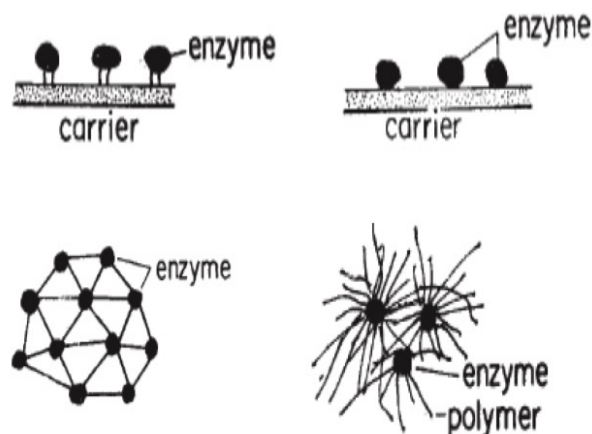


Figure 2.17: Immobilisation methods. From left top to right bottom: covalent bonding, adsorption, cross-linking and entrapment (figure taken from [30]).

The first method, which is the most studied method of all, consists of making a covalent link between the functional groups of the enzyme and the carrier. The reaction used to connect the enzyme to the carrier will depend on the enzyme's functional groups (e.g. hydroxyl groups, carboxyl groups, amino groups). Some of the most common reactions are acylation, arylation, alylation. However, sometimes it might be necessary to use a cross-linking agent, which will connect to both the enzyme and the carrier. One of the most used cross-linking agents is glutaraldehyde [30].

The covalent bounding allows an easy coupling of the enzyme to the carrier, prevents the possibility of leakages of the attached enzymes, and presents an enzyme-carrier system that is easy to handle. On the other hand, the matrix and the enzyme can not be renewed, and there is a possible loss of activity.

The second method makes use of physical adsorption (i.e. through Van der Waals forces, hydrogen or hydrophobic bonding) or by ionic binding. By altering some of the immobilisation conditions (e.g. pH, temperature) it is possible to detach the enzyme from the carrier (i.e. a reversible immobilisation). This process operates in mild conditions avoiding the inactivation of the enzyme, however, if the attachment between the enzyme and the carrier is not strong enough, it might occur some enzyme leakage. The most commonly adsorbents used are alumina, bentonite, calcium carbonate, among others [30].

The cross-linked enzymes (CLEs) can be divided in two separate groups: cross-linked enzyme aggregates (CLEAs) and cross-linked enzyme crystals (CLECs). The method to produce CLECs crystallises the enzymes and afterwards links the crystals with the help of glutarelddehyde. Despite being very stable and resistant to aggressive conditions (e.g. heat, organic solvents) the crystallisation process is long, costly and requires very pure enzymes. Therefore, it is no longer in use, and has been replaced by the production of CLEAs, which uses precipitation instead. By adding salts to an aqueous solution filled with proteins, precipitation will occur and the proteins will aggregate by non-covalent bonding without suffering denaturation. In the presence of a monomer that undergoes (co)polymerisation, the CLEA is modified enabling the formation of several different types of CLEAs as shown in figure 2.18. Moreover, it is a technique that has been applied to a wide range of hydrolases, oxidoreductases and lyases [21]. There are several advantages to this method: unlike the production of CLECs, it does not

require pure enzymes, can be obtained from crude enzyme preparations, does not require a carrier, achieves high catalyst productivities, and does not suffer denaturation.

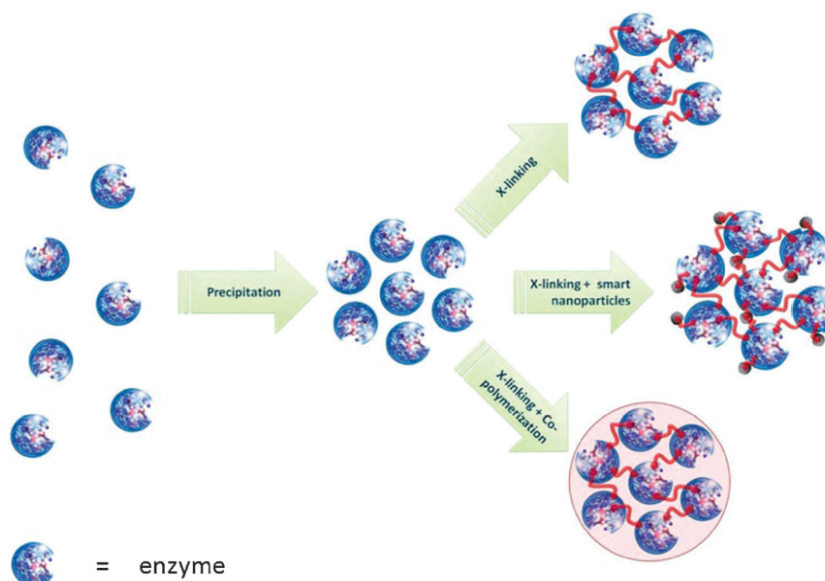


Figure 2.18: The different types of cross-linked enzyme aggregates, CLEAs (figure taken from [21]).

Entrapment comprises the trapping of the enzyme on the carrier. No chemical reaction occurs between the enzyme and the carrier, being that the carrier is fabricated while the entrapment process runs. The most common used carriers are silica sol gels and hydrogels. This process is quite simple, does not require large quantities of the enzyme, and there is very little change of flavoring it. Nevertheless the enzyme can easily flow away from the carrier.

The carrier is essential for the performance of the immobilised enzyme, therefore its important to think thoroughly on its choice. The carriers can be divided in two groups according to their chemical composition: organic and inorganic carriers. The organic carriers are divided in natural and synthetic polymers. Polysaccharides (e.g. cellulose, chitin, starch) and proteins (e.g. collagen, albumin) are examples of natural polymers; while polystyrene, polyamides are some examples of synthetic polymers. Silica, zeolites and mesoporous silicas are some examples of inorganic carriers. Good carriers are known for being hydrophilic, resistant to microbial attack, biocompatible, for withstanding compression, and for possessing a large surface area to facilitate the contact between the enzyme and the substrate [30].

With the discovery and development of these methods, it became possible to apply them in several fields such as medicine, food industry, drug metabolism, among others [30].

In order to evaluate the outcome of the immobilisation of enzymes, three parameters are taken into account: immobilisation yield, immobilisation efficiency and the activity recovery [21]. This immobilisation yield gives the percentage of the total enzyme activity present in the enzyme after being immobilised. To calculate the immobilised activity, one needs to subtract the immobilised enzyme activity from the total

activity of the free enzyme.

$$\text{Immobilisation yield (\%)} = 100 \times \frac{\text{immobilised activity}}{\text{starting activity}} \quad (2.6)$$

The immobilisation efficiency expresses the percentage of the bound enzyme that remains in the solution after the immobilisation.

$$\text{Immobilisation efficiency (\%)} = 100 \times \frac{\text{observed activity}}{\text{immobilised activity}} \quad (2.7)$$

The value of immobilisation efficiency can be 0%, if no activity is found in the immobilisate.

The activity recovery gives an idea of the overall success of the immobilisation process.

$$\text{Activity recovery (\%)} = \frac{\text{observed activity}}{\text{starting activity}} \quad (2.8)$$

The value of the observed activity varies accordingly with the type of activity trial, such as the type and concentration of substrate, temperature, pH, as well as with the physical characteristics of the biocatalyst (particle size, pore size, hydrophilicity-hydrophobicity).

2.4.1 Single-step EDC coupling method

In this work, the enzyme, xylanase, is attached to the cellulose beads by a covalent bond. It requires the use of a cross-linking agent, EDC (1-ethyl-3-(3-dimethylaminopropyl) carbodiimide hydrochloride), figure 2.19.

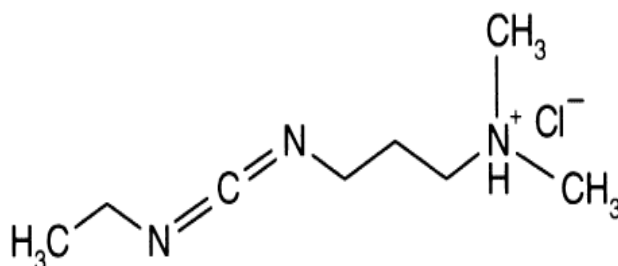


Figure 2.19: Chemical structure of EDC (figure taken from [31]).

EDC is a zero-length crosslinker (i.e. no additional structures such as spacer atoms are added to the formed bond), that covalently links the carboxyl groups of one molecule to the amino groups of another molecule, forming an amide bond between the two. This type of crosslinkers does not belong to the final carrier-protein complex that is formed. It is a heterobifunctional crosslinker, since it has two different reactive groups at each end. This way it is possible to make the two reactive groups specific for a certain protein, making sure that only the desired protein attaches to it.

The crosslinkers are chosen according to their solubility, length and reactivity. In this case, it was of interest to find a crosslinker that would react with carboxyl groups (-COOH), as well as be soluble in water in order to perform the immobilisation in aqueous conditions. The single-step EDC coupling method is as follows:

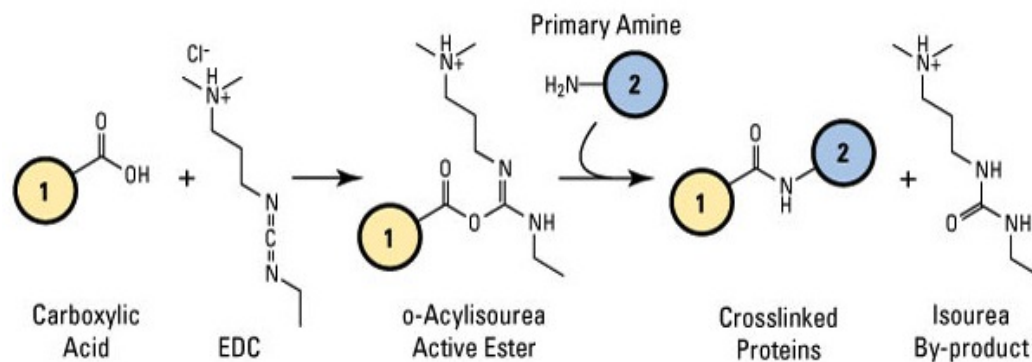


Figure 2.20: Reaction scheme using EDC as crosslinker (figure taken from [32]).

Figure 2.20 shows that the EDC reacts with the carboxylic acid to form an activated *O*-Acylisourea intermediate. The protein containing the amino group will react with the intermediate and form an amide bond with the initial carboxyl groups. The crosslinked molecules are obtained as well as a soluble urea derivative, a by-product of the reaction.

Chapter 3

Experimental

In this chapter, a more exhaustive explanation of the methods and materials used for the execution of this research is presented. Firstly, TEMPO oxidation, used to convert the primary hydroxyl groups (-CH₂OH) of the cellulose beads into carboxyl groups (-COOH) is addressed, followed by the conductometric titration, which quantifies the amount of formed carboxyl groups. Also, the oxidised beads were examined with an FTIR spectrophotometer to confirm (qualitatively) the success of the oxidation. Single-step EDC coupling was used to immobilise the enzyme (xylanase), onto the cellulose beads, followed by the Bradford protein assay, in order to determine the amount of enzyme that coupled to the cellulose beads. Lastly, the catalytic activity was calculated.

3.1 TEMPO oxidation of cellulose beads

3.1.1 Material

For this experiment, cellulose beads were provided by the Åbo Akademi University, Turku, Finland (figure 3.1). TEMPO 98 % (w/w) (2,2,6,6-tetramethyl-piperidin-1-yl)oxyl was purchased from Sigma-Aldrich, sodium hypochlorite (NaClO) 10-15 % (w/v), sodium chlorite (NaClO₂) 80 % (w/w) and monosodium dihydrogen phosphate dihydrate (NaH₂PO₄·2H₂O) ≥ 99 % (w/w) were available in the laboratory.

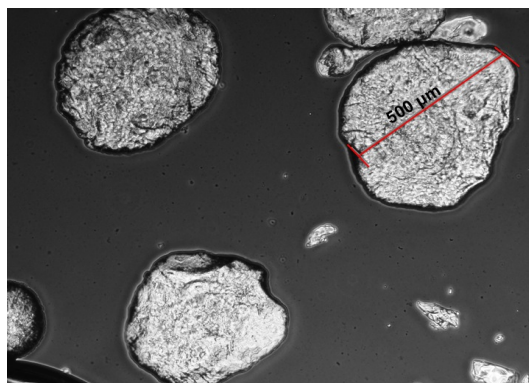


Figure 3.1: Image of the cellulose beads seen through the microscope. The beads have a diameter of approximately 500 µm.

3.1.2 Equipment

Microscope OLYMPUS IX83. Sartorius Secura scale (0.00001 g resolution) was used to weigh all the reagents and cellulose samples, the pH was measured with pH meter HI 2020-02 by HANNA, and the conductivity with HQ40d Portable pH/Conductivity meter. The water-bath with agitation, Julabo SW22 (figure 3.2), was used for the TEMPO oxidation.



Figure 3.2: Water bath Julabo SW22. (figure taken from [33]).

3.1.3 Method

Four samples (sample 1 to sample 4) of wet cellulose beads of approximately 10 g each were added in 4 different volumetric flasks. To each flask 100 ml of 50 mM NaH_2PO_4 buffer pH 5.3 was added. The beads and the buffer were left overnight. The next morning, the reagents NaClO_2 , TEMPO and NaClO were added, in this exact order, to each flask.

As explained in the section 2.2.3.1, the main goal of this experiment is to transform the primary hydroxyl groups ($-\text{CH}_2\text{OH}$), present on of the cellulose beads, to carboxyl groups ($-\text{COOH}$). According to the protocol followed by Trivedi et al. [34] an increase in the quantity of carboxyl groups on the beads is obtained when the quantities of NaClO_2 are increased for each sample, while the other two reagents,

TEMPO and NaClO, are added in the same quantities to all samples. Table 3.1 shows the required quantities of reagents for each sample.

Table 3.1: Amount of reagents used for the TEMPO oxidation (mmol.g⁻¹ cellulose beads).

Reagents	Samples			
	Sample 1	Sample 2	Sample 3	Sample 4
NaClO ₂	1.50	3.10	7.40	12.3
TEMPO	0.200	0.200	0.200	0.200
NaClO	0.600	0.600	0.600	0.600

The oxidation was performed in the water-bath at 60° C for 5 h, at an agitation of 100 rpm. Once the oxidation was finished, the pH of each sample was measured and the beads were washed with ultra-pure water Sartorius Stedim until the conductivity was below 10 µS.cm⁻¹ to make sure that there were no residual salts on the beads.

3.2 Fourier Transform Infrared Spectroscopy

3.2.1 Materials

Oxidised cellulose beads with different amounts of carboxyl groups, and non-oxidised cellulose beads were analysed.

3.2.2 Equipment

Perkin Elmer Spectrum 100 FT-IR spectrophotometer was used to measure the absorbance.

3.2.3 Method

Fourier Transform Infrared Spectroscopy was used to verify if the TEMPO oxidation had been accomplished. This technique allows to confirm the presence of the carboxylic groups formed on the cellulose beads by irradiating them with infrared light and by looking at the absorption spectra of the tested four samples.

In Infrared spectroscopy a sample is irradiated with infrared light. This light is partially absorbed by a part of the sample at a certain frequency, forming a peak on the spectrum which corresponds to the frequency of the atoms' vibration. It is important to outline that the vibrations can cause a change on the bond angle (i.e. *bending*) or a change in the bond length (i.e. *stretching*). According to the wavenumber at which the peak appears, it is possible to know to which atoms it corresponds enabling one to confirm which bonds exist in the sample. To obtain the final spectra it is necessary to use the Fourier transforms.

3.3 Conductometric titration

3.3.1 Materials

Hydrochloric acid 37 % (HCl) (v/v) and sodium hydroxide ≥ 98 % (NaOH) (w/w) were purchased from Merck. Sodium chloride ≥ 99.5 % (NaCl) (w/w) was purchased from VWR. The oxidised cellulose beads were available in the laboratory.

3.3.2 Equipment

S470 Mettler Toledo Seven Excellence™ pH/Conductivity meter is equipped with InLab Expert Pro ISM electrode and InLab 738 ISM conductometric sensor (figure 3.3).



Figure 3.3: S470 Mettler Toledo Seven Excellence™ pH/Conductivity meter (figure taken from [35]).

3.3.3 Method

This experiment allows to quantify the amount of carboxyl groups obtained during the TEMPO oxidation, on the cellulose beads. The standard protocol SCAN-CM 65:02 was used [36], with slight changes. After the oxidation, the beads are transformed to proton form, i.e. all the groups receive a positive hydrogen as counter-ion (they are protonised). To do that, the beads were suspended at 0.01 g.ml⁻¹ concentration (i.e. 100 ml of HCl for 1 g of beads) in a 100 mM HCl solution for approximately 30 minutes. The protonisation reaction that took place is as follows: cellulose-COONa + HCl ! cellulose- COOH + NaCl. Afterwards, the obtained solution was titrated with a 10 mM NaOH solution at the rate of 0.1 ml.min⁻¹. At each addition of NaOH solution, the conductivity was measured. The titration reaction is the following: Cellulose-COOH + NaOH ! Cellulose-COO⁻ Na⁺ + H₂O. Sodium chloride was added to the solution in order to improve the accuracy of the conductivity measurements. The beads were freeze dried, before titration, to determine the dry weight that was used in the experiment. A plot conductivity (?S.cm⁻¹) vs volume of NaOH (ml) similar to figure 3.4 should be obtained.

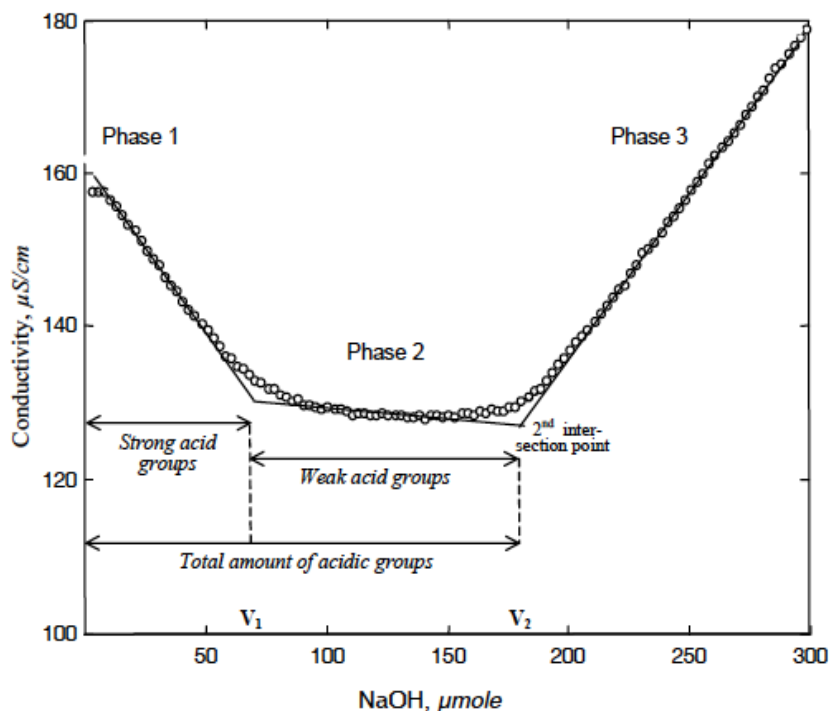


Figure 3.4: Conductivity ($\mu\text{S}\cdot\text{cm}^{-1}$) vs volume of NaOH (ml) (figure taken from [36]).

The conductometric titration allows to determine the acidic groups present in solution if the used volume of NaOH is known. The decrease in conductivity represents the neutralisation of the acidic groups. Phase 1 corresponds to the neutralisation of the strong acidic groups, phase 2 corresponds to the neutralisation of the weak acidic groups and phase 3 represents an accumulation of NaOH. If there are no strong acidic groups in solution, which is the case, the decrease of conductivity is due to the neutralisation of the protons liberated by the sodium chloride. Therefore, the quantity of carboxyl groups present on the cellulose beads was calculated according to the used volume of NaOH in phase 2, as illustrated by the following equation:

$$\text{Amount of carboxyl groups (mmol}\cdot\text{g}^{-1}) = \frac{C \times \Delta V}{m} \quad (3.1)$$

where ΔV is equal to V_2 minus V_1 which represents the used volume (ml) of 10 mM NaOH solution to titrate the existing weak acid groups (-COOH); C is the concentration of the solution of NaOH ($\text{mmol}\cdot\text{ml}^{-1}$), and m is the weight of the freeze dried beads in (g).

3.4 Single-step EDC coupling

3.4.1 Materials

Xylanase (endo-1-4- β -Xylanase), X302, was purchased from MetGen Oy, Helsinki. EDC (1-ethyl-3-(3-dimethylaminopropyl) carbodiimide hydrochloride) $\geq 98\%$ (w/w) was purchased from Sigma-Aldrich.

Trizma base (2-Amino-2-(hydroxymethyl)propane-1,3-diol) ≥ 99.9 % (w/w), and di-sodium hydrogen phosphate dihydrate ($\text{Na}_2\text{HPO}_4 \cdot 2\text{H}_2\text{O}$) ≥ 98 % (w/w), hydrochloric acid (HCl) 37 % (v/v) were available in the laboratory. The oxidised cellulose beads were ready for use.

3.4.2 Equipment

Grant Bio PTR60 360° Vertical Multi-Function Rotator (figure 3.5) was used for the thorough mixing of the content of the microtubes containing the enzyme and the cellulose beads.



Figure 3.5: Grant Bio PTR60 360° Vertical Multi-Function Rotator (figure taken from [37]).

3.4.3 Method

As described in section 2.4.1, the main goal of this single-step EDC coupling method is to attach the enzyme, xylanase, on the cellulose beads. In order to have a successful immobilisation, the pH of the buffers used in this experiment should not exceed 7.5 [31]. Therefore, one buffer solution of 50 mM $\text{Na}_2\text{HPO}_4 \cdot 2\text{H}_2\text{O}$ pH 6.3 was prepared, as well as a buffer of 100 mM Tris-HCl solution pH 6.6.

Approximately 1 g of the oxidised cellulose beads from each of the 4 samples (sample 1 to sample 4) were placed in 4 respective tubes of 20 ml (tube 1 to tube 4). The cellulose beads were washed with 5 ml of 50 mM $\text{Na}_2\text{HPO}_4 \cdot 2\text{H}_2\text{O}$ buffer, for three consecutive times. In the meantime, xylanase was dissolved in the same buffer (this solution was designated as E_1). Knowing that in 5 ml of the solution, 1 mg of enzyme was needed, and that the 1 l original xylanase solution had 10 g of enzyme, then 960 μl of xylanase was dissolved in 48 ml of 50 mM $\text{Na}_2\text{HPO}_4 \cdot 2\text{H}_2\text{O}$ solution. To the tubes 1 to 4, 5 ml of 50 mM $\text{Na}_2\text{HPO}_4 \cdot 2\text{H}_2\text{O}$ solution and 5 ml of E_1 were added. The amount of EDC added to each tube bears a 1:1 relation with the quantity of carboxyl groups present on the beads.

Table 3.2 shows the needed quantity of EDC. It is important to underline that the quantity of EDC should have been calculated correspondingly with the amount of the carboxyl groups present on the beads after oxidation. However, since the conductometric titration was not performed at KU Leuven, it

was not possible at the time, to quantify the carboxyl groups. Therefore, the amount of EDC required for the single-step EDC coupling method was calculated according to the quantity of carboxyl groups reported in the literature [34].

Table 3.2: Quantity of EDC (g) required for xylanase immobilisation assuming the same quantity of COOH groups as reported in [34].

Reagent	Samples			
	Sample 1	Sample 2	Sample 3	Sample 4
EDC	0.110	0.120	0.190	0.260

The samples were left reacting for 2 h. Afterwards, the supernatant of each sample was transferred to 20 ml tubes (S_1 to S_4), and the beads were washed three times with a solution of 100 mM Tris-HCl. Figure 3.6 illustrates all the procedure explained above.

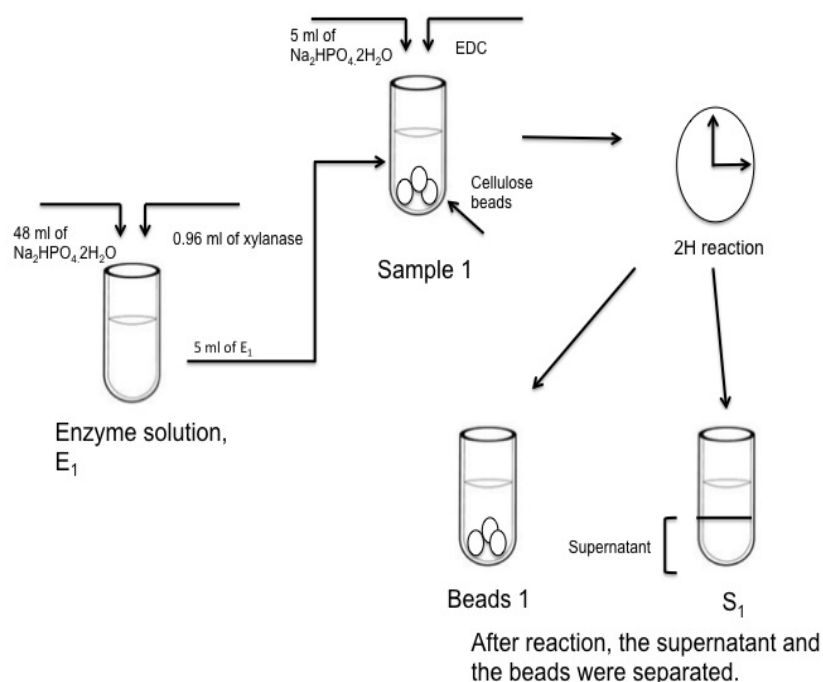


Figure 3.6: Illustration of the single-step EDC coupling method. Same procedure made for the remaining samples (i.e sample 2, 3, and 4).

3.5 Bradford protein assay

3.5.1 Materials

Bovine serum albumin (BSA) protein standard 200 mg/ml and Bradford reagent 0.1-1.4 mg/ml protein, also known as Coomassie Brilliant Blue G-250, were purchased from Sigma-Aldrich.

3.5.2 Equipment

The DR 5000™ UV-Vis Spectrophotometer was used to measure the absorbance of the tested samples. The light irradiated on the samples is ultra-violet.

3.5.3 Method

The Bradford protein assay is a colorimetric assay that allows to calculate the protein concentration (mg.l^{-1}) in a solution, by means of absorbance reading. The dye, Coomassie Brilliant Blue will bind in acidic pH to the amino acids of the protein, mainly histidine, arginine, tyrosine, phenylalanine and tryptophan, stabilising its anionic form, and allowing to quantify the protein in solution. In order to that, first it is necessary to obtain a standard curve (i.e plot absorbance vs concentration (mg.l^{-1}) using known protein standards. This plot allows to determine the concentration of protein in solution, when the respective absorbance is known. Normally, the closer the properties of the standard protein to the ones of the enzyme tested (in this case, xylanase) the more reliable the results are. However, due to the difficulty of finding such protein, the use of a standard protein bovine serum albumin (BSA) and gamma globulinbovinum, which are considered to give trustworthy results are used in such situations. For this research, BSA was used as protein standard (see Appendix B).

The supernatants (1 to 4) and the enzyme solution (E_1) were tested. All samples were diluted 20-fold since this method only measures below 20 mg.l^{-1} , and to each tube $500 \mu\text{l}$ of Coomassie Brilliant Blue G-250 was added.

3.6 Assay of endo-1-4- β -xylanase activity

3.6.1 Material

S-AXBL, Azo-xylan from birchwood dyed in Remazolbrilliant Blue R liquid, was acquired from Coring System Diagnostix GmbH. Di-sodium hydrogren phosphate dihydrate ($\text{Na}_2\text{HPO}_4 \cdot 2\text{H}_2\text{O}$) $\geq 98 \%$ (w/v), hydrochloric acid HCl 37 % (v/v) and ethanol 99.5 % (v/v) were available in the laboratory.

3.6.2 Equipment

A thermomixer F1.5 from Eppendorf, a centrifuge 5810R from Eppendorf, and a DR 5000™ UV-Vis Spectrophotometer, as shown in figure 3.7, were used for this experiment.



Figure 3.7: On the left (a): termomixer F1.5; on the right (b): centrifuge 5810 R; on the bottom (c): DR 5000TM UV-Vis Spectrophotometer (figures taken from [38] [39] [40]).

3.6.3 Method

In order to determine the enzyme activity, before immobilisation and after immobilisation, the protocol of Megazyme [41] was followed. After the single-step EDC coupling method, 0.5 ml of 100 mM $\text{Na}_2\text{HPO}_4 \cdot 2\text{H}_2\text{O}$ solution (buffer) and 0.5 ml of the substrate solution, azo-xylan, were added to the beads. The supernatant (S_1 to S_4) was diluted 2-fold i.e. 250 μl of the supernatant solution were mixed with 250 μl of the buffer, and the enzyme solution (E_1) was diluted 4-fold, i.e. 125 μl of the enzyme solution were mixed with 375 μl of the buffer. To all samples, 0.5 ml of azo-xylan was also added (figure 3.8). Hence, xylanase depolymerised xylan producing low and high-molecular weight fragments of the original xylan backbone.

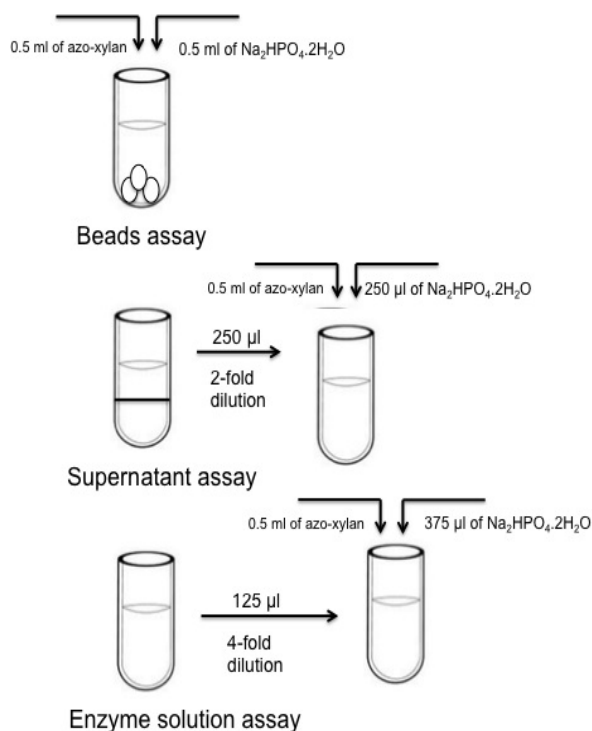


Figure 3.8: Illustration of the assay of endo-1-4-β-xylanase activity. The same procedure was done for the remaining samples.

Subsequently, all prepared samples were placed in the termomixer for 10 minutes, followed by the addition of 2.5 ml of ethanol. Afterwards, the samples were centrifuged (10 minutes) in order to remove the high molecular weight fragments, while the supernatant (low molecular weight fragments) of each sample was poured in a cuvette. The absorbance of the supernatant (i.e. the amount of incident light that is absorbed by the solution) was measured at 590 nm by the DR 5000™ UV-Vis Spectrophotometer. In order to measure the absorbance it was necessary to prepare, beforehand, a blank solution by adding 2.5 ml of ethanol, 0.5 ml of the substrate solution (azo-xylan) and 0.5 ml of the enzyme solution. The blank solution contains no analyte of interest, and it is used to calibrate the spectrophotometer.

The absorbance values were used in the MegaCalc™ provided by the Megazyme website (www.megazyme.com) in order to obtain the respective catalytic activities. For this, it was necessary to choose in the first place the source of xylanase. Due to the unknown culture in which xylanase was obtained, and from the list of fungus to choose from (*Trichoderma Longibrachiatum*, *Aspergillus niger*, *Humicola insolens*), the fungus *Aspergillus niger* was chosen since it is the most common of the three. Equation 3.3 of the standard curve of *Aspergillus niger* on Azo-xylan birchwood, provided in the Megazyme protocol, allows to calculate the endo-xylanase mU/assay.

$$\text{mU/assay (i.e. per /0.5 ml)} = 66.6 \times \text{Abs}^2 + 105 \times \text{Abs} + 3.9 \quad (3.2)$$

where Abs is the measured Absorbance of each sample .

To obtain the catalytic activity (U.g⁻¹ xylanase), the extraction volume and the dilution steps must

be taken into account. The extraction volume refers to the total volume of the initial solution. In this case, for both the free enzyme and the 4 samples of immobilised enzyme on the cellulose beads, the extraction volume is the same i.e. the total volume of the enzyme solution (E_1), 50 ml. The free enzyme was diluted 4-fold, and the 4 tested samples were diluted 2-fold. These dilutions were performed to ensure the correct reading of the absorbance in the spectrophotometer. This information was used on the following equation to determine the catalytic activity.

$$\text{U.g}^{-1} \text{ xylanase} = \text{mU/assay} \times 2 \times \text{extraction volume} \times \frac{1}{1000} \times \text{Dilution} \quad (3.3)$$

where 2 represents the conversion for 0.5 ml to 1.0 ml , and $\frac{1}{1000}$ is the conversion of milli-Units to Units.

Chapter 4

Results and Discussion

Firstly, the results of the TEMPO oxidation performed on the cellulose beads are addressed and compared with the ones from Trivedi et al. [34] which serve as a reference in this study. Conductometric titration allows to quantify the amount of the -COOH groups formed on the cellulose beads (quantitative results). Moreover it is also possible to confirm if the oxidation was successful by looking at certain parameters such as the colour of the samples, the pH and the Fourier Transformed Infrared (FTIR) spectra (qualitative results). Lastly, to confirm if the single-step EDC coupling method was successful the following techniques were used: the assay of endo-1-4- β -xylanase activity to determine the catalytic activity and the Bradford test to determine the protein concentration in solution. Both these methods allowed to analyse the results and withdraw conclusions regarding the immobilisation.

4.1 TEMPO oxidation of cellulose beads

4.1.1 Qualitative results

According to Trivedi et al. [34], it is possible to verify that the oxidation was successful by the colour and pH of the samples that were oxidised. As explained in section 3.1, the same quantities of the reagents NaClO and TEMPO were added to the 4 samples containing cellulose beads. The added quantity of NaClO₂ increased from sample 1 to sample 4. The colour of the samples should go from a light yellow to a dark brown with the increase of NaClO₂ added to each sample. The pH should remain acidic but with a slight increase from sample 1 to sample 4. Figure 4.1 shows the colour of the samples obtained after 5h of oxidation at 60° C in the water bath.



Figure 4.1: Samples 1 to 4 (left to right) of the oxidised cellulose beads. The NaClO_2 increases from left (i.e. sample 1) to right (i.e sample 4) of the oxidised cellulose beads.

Table 4.1 shows the values of pH obtained and the values reported in [34].

Table 4.1: Comparison of the pH values reported in the literature [26] with the ones obtained in this study.

pH	Samples			
	Sample 1	Sample 2	Sample 3	Sample 4
pH values reported in [34]	3.60	4.30	4.40	4.90
pH values of the experiment	4.56	5.05	5.90	5.98

Similarly as in Trivedi et al. [34], the obtained results show an increasing pH from sample 1 to 4, despite a discrepancy of the actual pH values themselves. The colour of the samples matches with the description of the protocol followed, and the slightly higher values in this work can be due to the pH of the used buffer, which was more basic compared with the reference (i.e pH of $\text{NaH}_2\text{PO}_4 \cdot 2\text{H}_2\text{O} \approx 4.6$ and 5.4 of the literature and the research, respectively).

Fourier Transformed Infrared Spectroscopy (a technique that grants an infrared spectra of absorption of the liquid solutions tested) was also studied. This technique allowed to compare the spectra of the reference cellulose beads (i.e. the ones that were not oxidised) with the oxidised cellulose beads (figure 4.2).

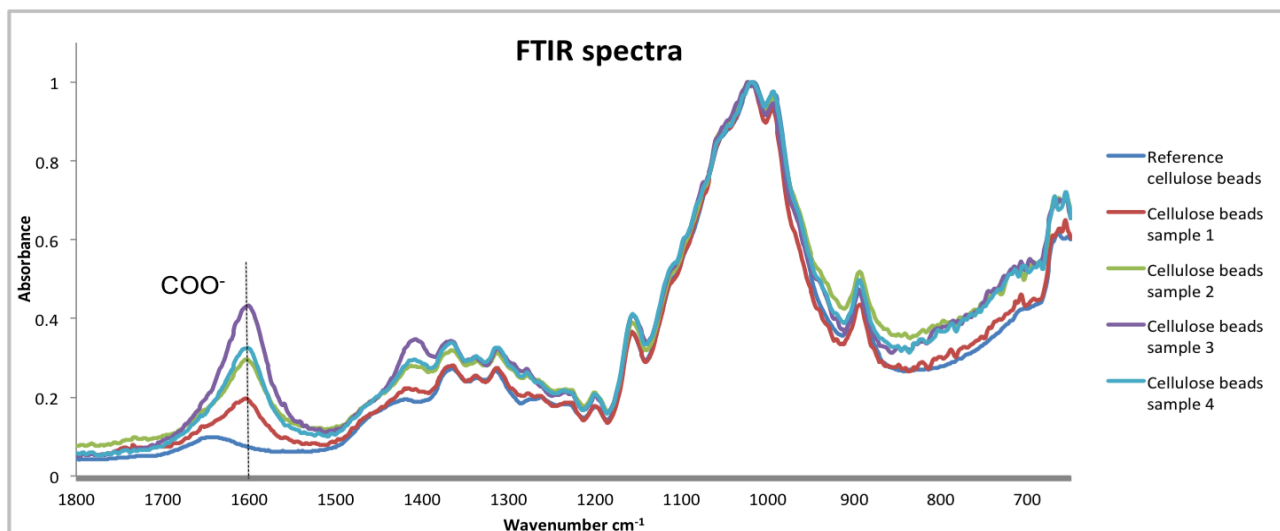


Figure 4.2: Fourier Transformed Infrared Spectra of the reference and oxidised cellulose beads. A characteristic peak of the carboxyl acid salt at 1600 cm^{-1} is evident for samples 1 to 4, which is absent for the reference cellulose beads.

As can be seen in figure 4.2, there is a clear difference between the spectra of the oxidised and non-oxidised cellulose beads. The Infrared spectra show for the oxidised beads, sample 1 to sample 4, a peak of the COO^- stretching band of the carboxylate (the carboxylic acid salt) at approximately 1600 cm^{-1} , while the Infrared spectrum of reference cellulose beads does not. This observation is consistent with the literature [42], which has measured the COO^- stretching band between $1610\text{ -}1550\text{ cm}^{-1}$. The non-oxidised beads show no peak in that region, indicating a clear effect of the oxidation reaction.

It is also possible to verify that the intensity of the peaks changes according to the samples i.e sample 3 shows the highest COO^- peak, followed by sample 4, 2 and 1. This outcome demonstrates that sample 3 has more carboxylic groups followed by sample 4, 2, and 1. This fact can be verified by the results of the conductometric titration which are explained next.

All of these results exhibit that the oxidation was successful, however they are insufficient to quantify the amount of formed carboxylic groups. Therefore, a quantitative method is described in the following subsection.

4.1.2 Quantitative results

Conductometric titration was performed as described in section 3.3. The results of the first sample are analysed in this sub-section, and the results of the remaining samples can be explored in Annex A. Figure 4.3 represents the V-shaped graph which shows the conductivity ($\mu\text{S}\cdot\text{cm}^{-1}$) vs used volume of NaOH (ml) of sample 1.

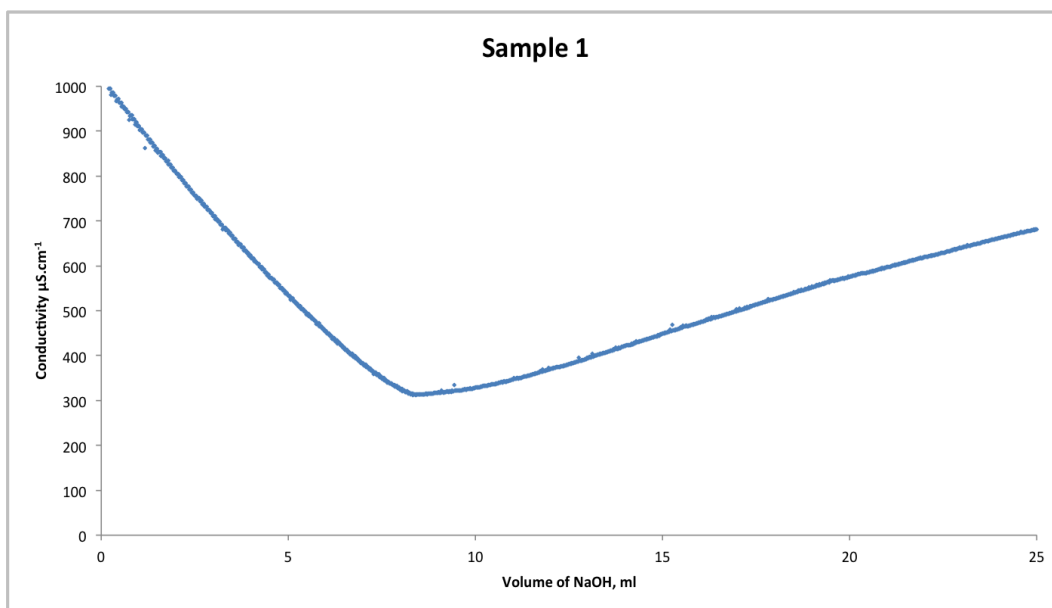


Figure 4.3: Conductometric titration graph of sample 1.

As highlighted in fig 3.4 it is possible to divide the V-shaped graph in three different zones. Zone 1 corresponds to the titration of the strong acid groups, which do not exist in this experiment. Therefore, the decrease of conductivity is due to the neutralisation of some released protons of the NaCl. Zone 2 is the one of interest since it matches to the titration of the weak acid groups, in this case the carboxyl groups (-COOH). In zone 3 there is an increase of conductivity due to the excess of NaOH. Zone 1, 2 and 3 were defined to maximise the R^2 (i.e. to maximise the linearity) in all 3 zones. Figures 4.4, 4.5, 4.6 represent zone 1, 2 and 3 of sample 1, respectively.

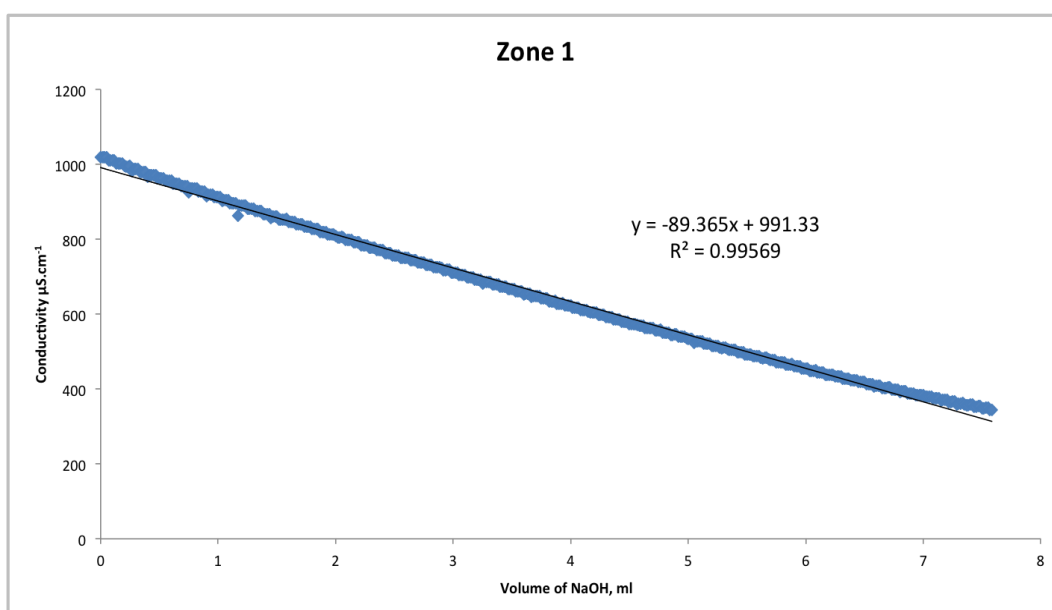


Figure 4.4: Zone 1 of the conductometric titration graph.

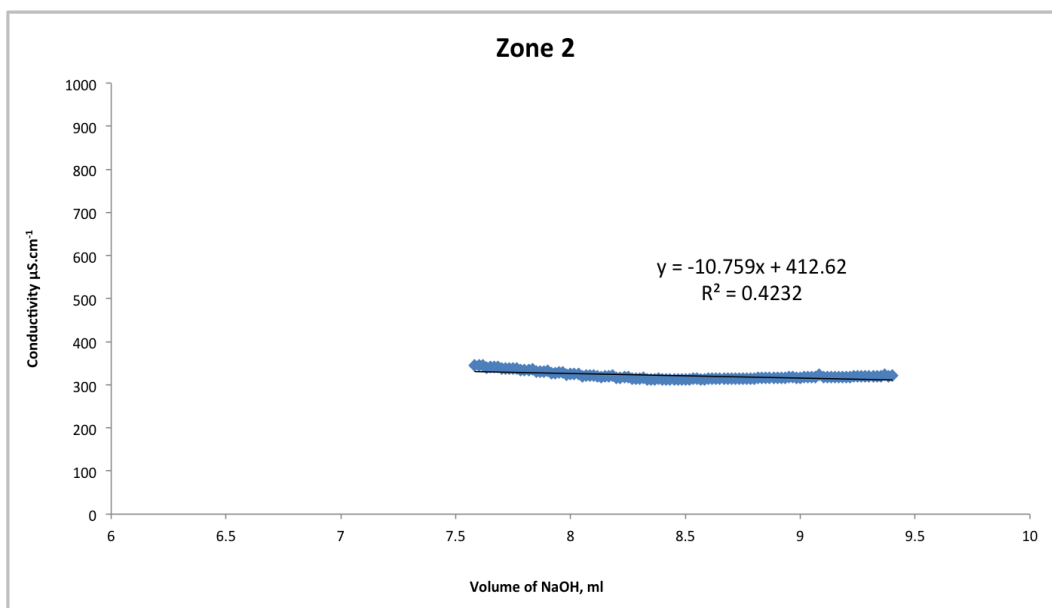


Figure 4.5: Zone 2 of the conductometric titration graph.

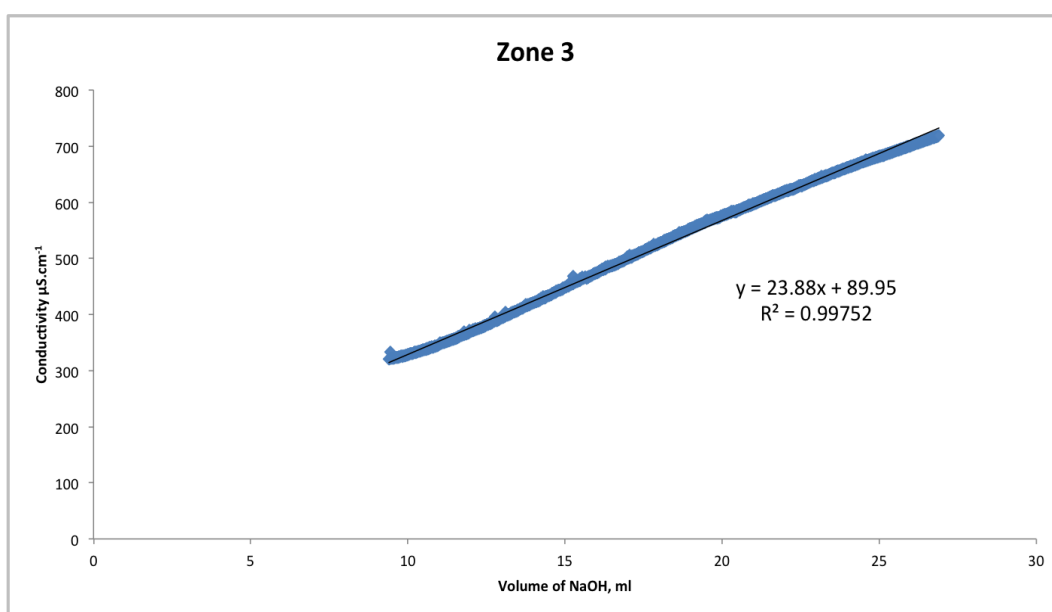


Figure 4.6: Zone 3 of the conductometric titration graph.

The volume of NaOH needed to titrate the carboxyl groups present on the cellulose beads is determined by the part of the curve in zone 2. Knowing the mass of dried beads and the concentration of the solution of NaOH (0.01 M), it is possible to calculate the quantity of carboxyl groups for all samples using equation 3.1. Table 4.2 lists the mass of the dried beads, volume of NaOH used for the titration and the amount of the carboxyl groups for samples 1 to 4.

Table 4.2: Amount of COOH groups (mmol.g^{-1}) determined by equation 3.1. The mass of dried beads (g), volume of NaOH (ml) and the concentration of NaOH (0.01 M) were used in the equation.

Samples	Mass of dried beads (g)	Volume of NaOH (ml)	Amount of COOH groups (mmol.g^{-1})
Sample 1	0.0584	1.85	0.316
Sample 2	0.0581	2.48	0.426
Sample 3	0.0627	3.40	0.542
Sample 4	0.0643	3.30	0.513

These results are quite interesting, since sample 3 has more carboxylic groups compared with sample 4. According to Trivedi et al. [34], the higher the amount of the reagent NaClO_2 used on the oxidation, the more carboxyl groups are formed. However, as can be seen in table 4.2, sample 4 to which a higher amount of NaClO_2 was added, has less carboxyl groups than sample 3. Regardless of this discrepancy, sample 1, 2 and 3 show the expected results since sample 2 has more carboxyl groups than sample 1, and sample 3 has more carboxyl groups than samples 1 and 2. It is hard to explain the reason for this outcome, although it could mean that, in these conditions, the quantities of the reagents used for sample 3 are present in the optimal ratio for the TEMPO oxidation. Also, the quantity of NaClO_2 used on sample 4 might have created a saturation effect i.e. no additional COOH groups are linked to the beads with further increase in NaClO_2 concentration.

Moreover, it is also important to stress the difference of these results compared with the ones of the literature as can be seen in table 4.3.

Table 4.3: Comparison of the quantity of carboxyl groups of the literature [34] with this research.

Samples	Amount of COOH groups (mmol.g^{-1}) reported in the literature [34]	Amount of COOH groups (mmol.g^{-1}) in this experiment
Sample 1	0.560	0.316
Sample 2	0.620	0.426
Sample 3	0.980	0.542
Sample 4	1.35	0.513

The significant difference between the results from literature and the ones in this work are most likely caused by the different structure of the beads. The beads used in the literature were prepared by dropping technique in a small lab scale, while the ones used in this work were also prepared by dropping technique, but freeze-dried afterwards in a large scale. The latter might have led to the production of stiffer beads and less open pores, hindering the penetration of the reagents. Regardless of the low amount of carboxyl groups comparatively with the ones of the literature, the single-step EDC coupling method was carried out either way.

4.2 Bradford protein assay

It is clear that the quantity of enzyme that attaches to the cellulose beads is related with the obtained catalytic activity. Therefore, the Bradford protein assay was performed to quantify the amount of enzyme that was coupled with the carboxyl groups of the cellulose beads and to correlate this with the catalytic activity explained in the following section with these values.

The amount of enzyme present on the enzyme solution (E_1) and on the supernatant of each sample after the reaction of the single-step EDC coupling method was determined. Table 4.4 presents the amount of enzyme calculated using the Bradford protein assay.

Table 4.4: Amount, in mg, of xylanase present on E_1 and the supernatant of samples 1 to 4.

Samples	Absorbance	Xylanase concentration ($\text{mg}\cdot\text{l}^{-1}$)	Xylanase mass (mg)
Xylanase solution (E_1)	0.558	200	9.6
Supernatant sample 1	0.395	81.1	0.811
Supernatant sample 2	0.390	76.6	0.766
Supernatant sample 3	0.371	59.8	0.598
Supernatant sample 4	0.374	62.5	0.625

The amount of xylanase that coupled with the carboxyl groups of the cellulose beads was calculated by subtracting the mass of supernatant in the sample from the mass of xylanase in solution (i.e. 1 mg). It is important to outline that from the enzyme solution, only 5 ml were transferred to the tube where the single-step EDC coupling method occurred, which means that the transferred mass of enzyme was only 1 mg. The results are listed in table 4.5.

Table 4.5: Amount, in mg, of xylanase attached to the carboxyl groups of the cellulose beads.

	Cellulose beads sample 1	Cellulose beads sample 2	Cellulose beads sample 3	Cellulose beads sample 4
mass of attached xylanase (mg)	0.190	0.234	0.402	0.375

The quantity of coupled enzyme was correlated with the catalytic activity, as explained in the next section.

4.3 Enzyme activity

4.3.1 Comparison between the catalytic activity of the free enzyme with the immobilised enzyme

Firstly, the catalytic activities of the free enzyme are compared with the catalytic activities of the immobilised enzyme. The single-step EDC coupling method was performed approximately 10 times per sample 1, 2, 3 and 4 (possibly excluding some outliers) on the same batch of oxidised beads in order to obtain a sufficient amount of data. The mean and standard deviation were computed for all samples except the removed outliers. Table 4.6 presents the mean and standard deviation of catalytic activity which was calculated using the method described in 3.6 obtained for every tested sample.

Table 4.6: Catalytic activity ($\text{U}\cdot\text{mg}^{-1}$ xylanase) of the free and immobilised xylanase.

Samples	Catalytic activity ($\text{U}\cdot\text{mg}^{-1}$ xylanase)
Free xylanase	13.4 ± 3.77
Immobilised xylanase sample 1	0.513 ± 0.254
Immobilised xylanase sample 2	0.528 ± 0.246
Immobilised xylanase sample 3	0.867 ± 0.083
Immobilised xylanase sample 4	0.761 ± 0.176

The immobilisation yield is the ratio of the individual xylanase activities after immobilisation and the mean of the activity of the free xylanase (i.e. $13.4 \text{ U}\cdot\text{mg}^{-1}$ xylanase). The immobilisation yield was calculated for at least 10 new, identical samples out of every of the 4 original samples (i.e. sample 1, 2, 3 and 4). Using equation 2.6 in chapter 2 the mean and standard deviation of the immobilisation yield are listed in table 4.7.

Table 4.7: Immobilisation yield of samples 1, 2, 3 and 4.

Samples	Immobilisation yield(%)
Immobilised xylanase sample 1	3.84 ± 1.90
Immobilised xylanase sample 2	3.95 ± 1.84
Immobilised xylanase sample 3	6.49 ± 0.624
Immobilised xylanase sample 4	5.70 ± 1.31

These results show a big difference between the catalytic activity of the free enzyme compared with the immobilised enzyme, more precisely a decrease of 97.3 %, 96.2 %, 93.8% and 95% of the catalytic activity of sample 1, 2, 3, and 4, respectively. Therefore, the yields are extremely low i.e. in all samples the yield is lower than 10%. On the other hand, the obtained values are in accordance with the amount of xylanase attached to the cellulose beads from table 4.5 since the samples that have have a smaller amount of xylanase attached to the cellulose beads, should have a lower catalytic activity such

as sample 1 and 2; while the ones with more xylanase attached to the cellulose beads should have a higher catalytic activity.

The immobilisation can be one of the reasons for the obtained catalytic activity results, since it can cause the loss of the enzyme's dynamic properties, alteration of the enzyme's conformation and reduce the access of the substrate to the enzyme's active centre [43]. Despite the reported successful attempts of immobilisation of a wide range of enzymes that show no significant decrease in the catalytic activity [44] [45], this hypothesis cannot be ruled out.

As mentioned in section 2.4, the success of enzyme immobilisation depends on the specificity of the carrier and method. Cellulose beads are considered appropriate carriers for enzyme immobilisation [4], however the carriers affect the orientation of the enzyme, which restricts the binding of the substrate or the cofactor (if it exists) to the active site [46]. Unfortunately, the available data does not allow to conclude whether the carrier influenced the chemical properties and/or conformation of the xylanase.

4.3.2 Occurrence of side reactions

The reagent EDC can undergo a range of side reactions that block the formation of the amide bond between the carboxyl groups of the cellulose beads with the amino groups of the xylanase. Figure 4.7 shows all the possible side reactions that can occur in the presence of EDC.

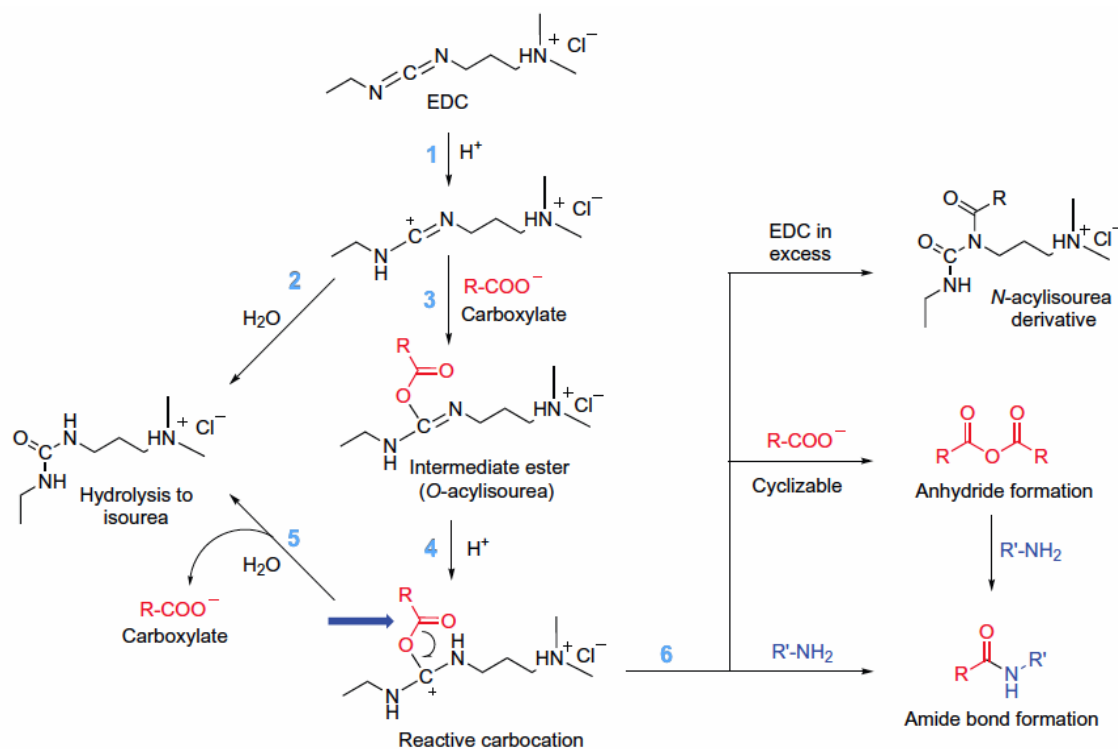


Figure 4.7: Possible side reactions of EDC that block the formation of the amide bond (figure adapted from [31]).

Path 1 illustrates the protonation of one nitrogen atom of the imine group (R_2CNR) of EDC resulting in the formation of an intermediate carbocation (i.e. the central carbon atom has a positive charge,

and 3 covalent bonds instead of 4). From here, there are two possibilities: or the desired intermediate, O-acylisourea, is formed due to the interaction with the carboxylate (R-COO⁻) (path 3); or it hydrolyses to isourea (path 2) which can not be used further. In case the O-acylisourea is formed, a reactive ester consequent of a second carbocation is produced (path 4). From this point forward, it is possible to produce the isourea by hydrolysis (path 5), or three other possible reactions are plausible (path 6). The reactive carbocation can react with the amino group of the enzyme and form the desired amide bond. In case there is excess of EDC relatively to the amount of carboxylates present, it is likely that the O-acylisourea will react with the secondary amines (RNHR) of the EDC yielding a *N*-acylisourea derivative, which is inactivate. Lastly, the intermediate ester can react with close-by carboxyl groups and form an anhydride. Luckily, it is still possible to form the amide bond if one of the carboxylates of the anhydride reacts with an amino group.

As can be seen, several possibilities can be the cause of an unsuccessful immobilisation. However, here, the production of *N*-acylisourea derivative can probably be rolled out as the only cause for the failed immobilisation. As explained in section 3.4 the amount of EDC used for the single-step EDC coupling method was determined according to the carboxyl groups reported in the literature [34]. Therefore, to know if it was used an excess of EDC it was necessary to compare the amount of EDC that was used for the immobilisation technique with the amount of EDC that should have been used. Table 4.8 shows the quantity of used EDC, the EDC that should have been used according to the (post hoc) results of the conductometric titration (table 4.3) and the percentual excess of EDC between these two.

Table 4.8: Comparison between the actual used quantities and post-hoc required quantities of EDC (g).

Samples	EDC required for this work (g)	EDC that should have been used in this work (g)	% Excess of EDC
Sample 1	0.110	0.0600	45.0
Sample 2	0.120	0.0820	31.6
Sample 3	0.190	0.104	45.0
Sample 4	0.260	0.0983	62.0

According to table 4.8 there is an evident use of excess of EDC. Figure 4.7 shows that the presence of excess of EDC in solution might lead to the production of *N*-acylisourea derivative, rendering the formation of the amide bond impossible. However, it seems unlikely since there is some (low) catalytic activity present after immobilisation. If the *N*-acylisourea derivative had been formed it would render the formation of the amide bond impossible which would lead in the extreme case to a catalytic activity of the immobilised enzyme approximately zero, and a catalytic activity of the supernatant equal to the one of the free enzyme, as expected. The catalytic activity of the supernatant has not been reported in this work since the results were too variable for samples prepared in the same way. Either way, the catalytic activity never surpassed the one of the free enzyme. As can be verified from table 4.6, the catalytic activity is low, but still significantly different from zero, meaning that the desired coupling of the carboxyl groups of the cellulose beads with EDC took place (although insufficiently), and that the formation of the

undesired *N*-acylisourea derivative probably occurred, but not completely. Moreover, the cross-linking (explained in the section below) most likely occurred as well, at the same time as these two reactions, and probably at a higher rate. Note that other side reactions might have occurred as well, but they are not further treated here.

4.3.3 Study to determine the occurrence of cross-linking

Despite of all these arguments discussed above, there is reason to believe that the unsuccessful immobilisation is result of the fact that xylanase has both carboxyl and amino groups in its composition, leading to the cross-linking (between the carboxyl and amino groups) of xylanase when in presence of EDC.

In order to verify the occurrence of cross-linking, a simple trial was performed (see figure 4.8). Instead of adding the EDC and enzyme solution to the cellulose beads in order to start the immobilisation, solely EDC in varying quantities (i.e. 0.114 g used in sample 1 and 0.266 g used in sample 2) and enzyme solution were added to different tubes. The occurrence of cross-linking can be detected by a significant decrease of the catalytic activity (since the enzymatic sites of xylanase take part in the cross-linking, and are hence no longer accessible to the substrate).

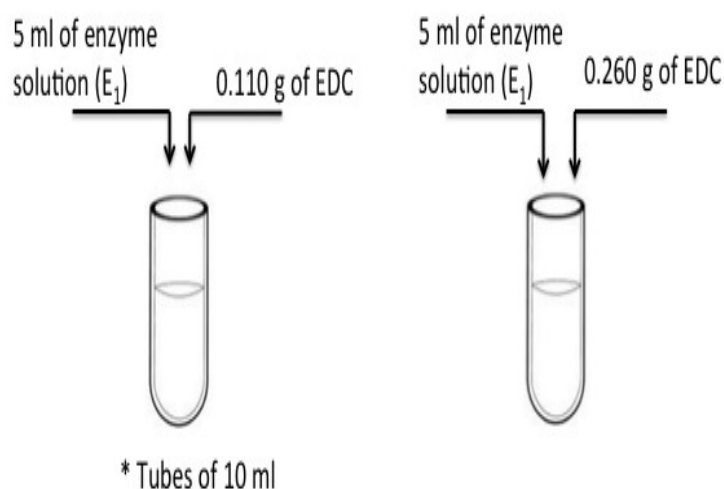


Figure 4.8: Scheme of the performed trial to prove the occurrence of cross-linking. EDC, in varying quantities, was mixed with enzyme solution to compare the catalytic activity of the free enzyme.

These two samples reacted for 2 hours, followed by the enzyme activity assay (the same steps as the ones listed in section 3.6 were followed). Table 4.9 presents the measured catalytic activity and mean deviation.

Table 4.9: Catalytic activity ($\text{U}\cdot\text{mg}^{-1}$ xylanase) of the xylanase with EDC.

Samples	Catalytic activity ($\text{U}\cdot\text{mg}^{-1}$ xylanase)
Xylanase + EDC (1)	1.38 ± 0.0310
Xylanase + EDC (4)	0.710 ± 0.00251

Comparing these results with the ones of the free enzyme from table 4.6 it is possible to draw conclusions. The catalytic activity decreased substantially, more precisely by 90.1% and 94.9% for samples xylanase + EDC (1) and (4), respectively. This fact implies the occurrence of cross-linking (all parameters were maintained constant between the two conditions except the quantity of EDC). In case the EDC in solution would not interact with the enzyme, the results of the catalytic activity should be equal to the ones of the free enzyme. On the contrary, these results prove that the EDC is interacting with the carboxyl groups of xylanase and forming the intermediate ester, which will afterwards couple with the amino groups of xylanase. The amino groups of xylanase are the ones that take part in the immobilisation (i.e. they couple with the *O*-Acylisourea intermediate to form the amide bond), while the carboxyl groups are the ones that attach to the substrate (i.e. in this case, xylan) allowing the enzyme to catalyse the reaction as explained in section 2.3.1.1. Since the carboxyl groups are occupied due to the cross-linking, the catalytic activity is compromised and it drops.

Comparing both samples, it is clear that a higher quantity of EDC is accompanied by a stronger decrease in catalytic activity - the quantity of EDC is anti-correlated with catalytic activity. This implies the occurrence of cross-linking, since it seems the only phenomenon capable of explaining this outcome. Since the desired reaction occurs to a much lesser extent than the cross-linking, it can be concluded that the latter reaction (or potentially other competing reactions) is thermodynamically favourable, i.e. has a greater drop in Gibbs energy. However, both the desired and undesired reactions go on simultaneously (although at different rates).

4.3.4 Analysis of the time-frame on the single-step EDC coupling

It seems plausible that the simultaneous addition of both EDC and enzyme solution, could have prevented the coupling of the EDC with the carboxyl groups present on the cellulose beads, and instead allowed the EDC to couple with the ones present on the xylanase, thereby preventing the amide bond formation (between the carrier and the enzyme), and provoking the cross-linking. Therefore, another experiment to try to identify the cause of the unsuccessful immobilisation was performed .

Instead of following strictly the single-step EDC coupling method explained in section 3.4, a small adaptation was made. In the initial protocol [31], the reagent EDC was added immediately after the addition of the enzyme solution. Alternatively, the EDC was added first and left to react with the cellulose beads for 2h. Afterwards, the enzyme solution was added to the solution and reacted for 2 hours more. Finally, the catalytic activity assay was carried out, to see if this separate addition of reagents improved the reliability of the desired reactions.

Figure 4.9 presents all steps of the conducted alternative single-step EDC coupling method.

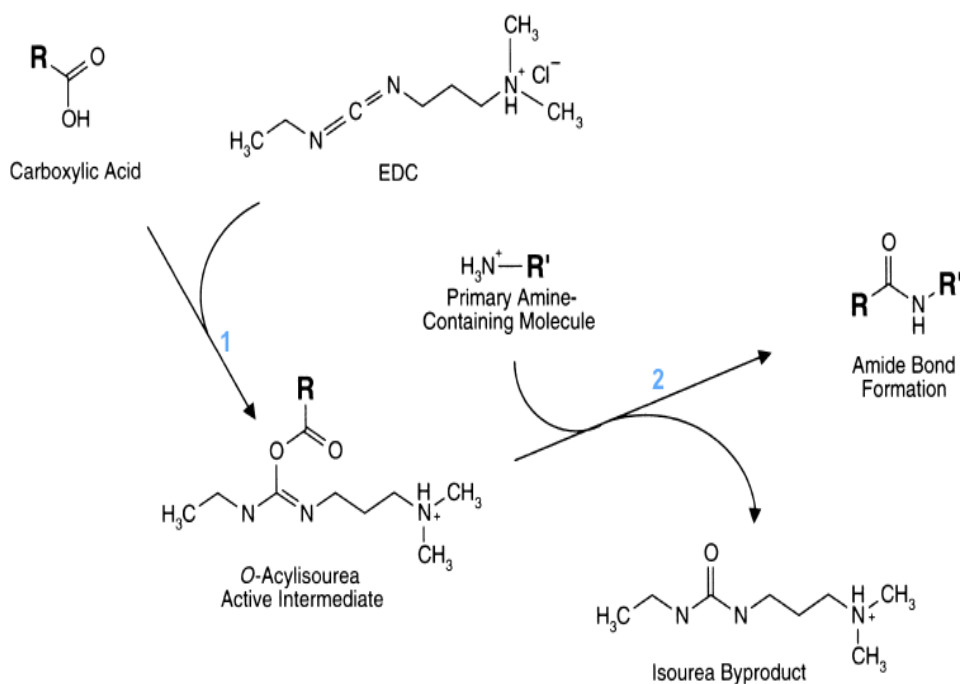


Figure 4.9: Scheme of the single-step EDC coupling method (figure adapted from [31]).

This approach had the objective to establish a more stable *O*-Acylisourea intermediate (path 1 of figure 4.9), making sure that the possibility of coupling of EDC with the carboxyl groups of the xylanase (once added to the solution) were lower, but instead the formation of the amide bond (between cellulose beads and xylanase) was greater (path 2 of figure 4.9). The measured catalytic activity is listed on table 4.10.

Table 4.10: Catalytic activity (U.mg⁻¹ xylanase) of the immobilised xylanase with a small modification (i.e. the EDC and the enzyme solution were added 2h apart) of the protocol.

Samples	Catalytic activity (U.mg ⁻¹ xylanase)
Immobilised xylanase sample 1	0.344
Immobilised xylanase sample 2	2.85
Immobilised xylanase sample 3	1.40
Immobilised xylanase sample 4	0.971

Unfortunately, this experiment was performed once, so it is difficult to say how reliable these values are. However, it is interesting to see that the catalytic activities of sample 2, 3 and 4 increased 440 %, 61.5 % and 27.6 %, compared with the ones of table 4.6, respectively, while the catalytic activity of sample 1 decreased 33 %. Nonetheless, it is difficult to make a straightforward comparison since the values of table 4.6 were averaged over more (approximately 10) trials while the values of table 4.10 are not. Hence, the reported activity values of the former are more reliable than the ones of the latter. In

case this approach had been performed more times and the interval of the results would be superior to the ones of table 4.6, then it would be possible to conclude that this path has higher yields than the one of the followed protocol. Moreover, it is unclear why the catalytic activity of sample 2 is so high compared with the remaining samples.

4.3.5 Mass-transfer effects

Besides all these parameters discussed above that might have had an influence on the obtained results, it is important to take into account that the yield of the enzyme activity after immobilisation is also dependent on mass-transfer effects. [47] An immobilised enzyme can only catalyse a reaction if the substrate reaches the catalytic sites of the enzyme by diffusion through the solution [48]. Afterwards, the formed products diffuse to the bulk solution. Thus, the combination of all these factors lead in practice to a lower substrate conversion rate when using immobilised enzymes than when using free enzymes. In order to avoid diffusional limitations and increase the catalytic efficiency, some measures should be taken such as the use of smaller carriers (promoting easy diffusion, and a large surface-to-volume ratio to maximise the access to the enzyme molecules), and do the binding of the substrate on the outer shell of the carrier.

Chapter 5

Conclusions

In the present work, TEMPO oxidation and catalytic activity of the cellulose beads were studied. As explained in section 3.1, TEMPO oxidation transforms the primary hydroxyl groups ($-\text{CH}_2\text{OH}$), present on the cellulose beads, into carboxyl groups ($-\text{COOH}$). Therefore, the success of this experiment was extremely important since the immobilisation of xylanase could not take place without the latter. The conductometric titration allowed to quantify the produced carboxyl groups of sample 1 to 4. Despite the discrepancy between these values and the ones of Trivedi et al. [34], it was not an impediment for the execution of the single-step EDC coupling method.

The enzyme immobilisation results show a decrease of 97.3 %, 96.2 %, 93.8 % and 95 % of the catalytic activity of sample 1 to 4, respectively, compared with the catalytic activity of the free enzyme. In section 4.3, possible causes for the insuccess of the single-step EDC coupling method were investigated. Despite of the high number of reported successful cases of immobilisation of enzymes on different carriers [44] [45], and the fact that cellulose beads are classified as extremely good carriers [4], the impact of immobilisation on catalytic activity should not be neglected. The chemical interactions that occur between the carrier and the enzyme cause changes in the conformation of the enzyme which might lead to a decrease of the catalytic activity. The production of the isourea by-product might also be a cause for the decreased catalytic activity. Moreover, the pH can also influence the reaction, in the sense that the amide bond is formed more easily between pH 4.5 and 7.5. However, the pH of the buffer used for the single-step EDC coupling method was between these limits which means that this parameter was likely not the bottleneck.

Given the data obtained throughout this work, the most believable cause for this insuccess is the chosen immobilisation method (i.e. single-step EDC coupling method). EDC is a zero-length crosslinker commonly used to activate carboxyl groups to conjugate with amino groups. Despite all the advantages of this reagent [32], it can lead to several unwanted situations when used alone for the immobilisation. The formed *O*-acylisourea, is an extremely unstable intermediate that is hydrolysed back to carboxyl groups if it fails to react with the amino groups. Moreover, several side reactions of the EDC can take place as exemplified in figure 4.8. As discussed in section 4.3, it was not possible to prove if some of these side reactions took place, except for the side reaction caused by the excess of EDC in solution.

It was verified that the amount of EDC used for the single-step EDC coupling method was higher than necessary. An excess of EDC of 45.0 %, 31.6 %, 45.0 % and 61.2 % was obtained for sample 1 to 4, respectively. Consequently, it was concluded that the formation of the *N*-acylisourea derivative might have occurred although not completely since the catalytic activity after immobilisation was not null (i.e. the EDC attached to the carboxyl groups on the cellulose beads).

Despite all these grounds addressed above, the main reason for the low catalytic activities seems to be the fact that xylanase has both carboxyl and amino groups in its composition. It seems that the EDC coupled with the carboxyl groups of xylanase forming the *O*-acylisourea, which in turn coupled with the amino groups of xylanase instead of the cellulose beads. The cross-linking of xylanase likely prevented the production of the amide bond between xylanase and the carboxyl groups present on the cellulose beads. However, it seems that this latter (desired) coupling still occurred, although in very low quantities as demonstrated by the results obtained in table 4.6.

The feasibility of the single-step EDC coupling method of xylanase on cellulose beads, which was the main goal of this thesis, has proven to be rather limited. Hence, future research must be developed to try to find away around this seeming bottleneck. In the next section, some ideas/suggestions for improvement are addressed.

5.1 Future Work

The results in this thesis have shown that a more appropriate method must be used for the immobilisation of xylanase on cellulose beads. For instance, a good candidate might be the two-step EDC/sulfo-NHS coupling method. The addition of the sulfo-NHS ester (*N*-hydroxysulfosuccinimide), an hydrophilic reactive group, to the EDC reaction creates a more stable and soluble active intermediate, which will easily attach to the amino group of xylanase. Moreover, the excess of EDC can be removed before adding the protein to the reaction medium, avoiding cross-linking in case the protein contains both amino and carboxyl groups, as well as the formation of the (undesired) *N*-acylisourea derivative. Figure 5.1 shows the reaction with EDC and sulfo-NHS ester.

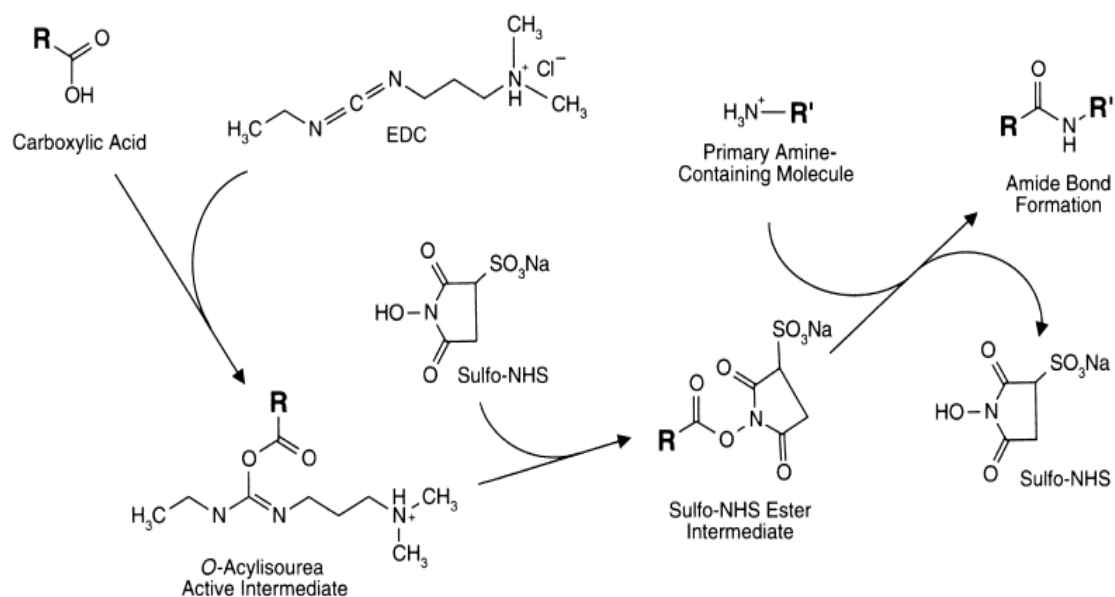


Figure 5.1: Two-step EDC/sulfo-NHS coupling method (figure taken from [31]).

Figure 5.1 indicates that the *O*-Acylisourea active intermediate formed by the reaction with the carboxylic acid and EDC will react with the sulfo-NHS to form the sulfo-NHS ester intermediate, more stable and soluble than the *O*-acylisourea. Subsequently, the formed intermediate will react with the primary amines yielding stable amide bonds. It is proven that the use of sulfo-NHS increases the efficiency and yield of the conjugation [31] [49].

Besides this, and taking into consideration that the results of table 4.10 are in average higher than the ones of table 4.6, it would be interesting to dig further into this to see if the different approach (i.e. the addition of the reagent EDC and the enzyme solution with 2h apart) used on this research in section 4.3, is productive.

The different immobilisation methods addressed in section 2.4 are also potential topics of future research. The covalent methods, which englobes the one used in this research, have been classified as the methods that enable the most stable (chemical) interaction between the enzymes and the carriers. However, the formation of these chemical bonds changes the structure of the enzymes leading, inevitably, to a decrease of the catalytic activity compared to the enzyme's free state. Moreover, it is a long and difficult process since it requires the functionalisation of the carrier, specific functional groups of the enzyme and a cross-linker. For this reason, perhaps the use of the physical immobilisation methods (such as adsorption and entrapment) would be a suitable alternative, since they retain the catalytic activity of the enzymes [50]. Comparing both examples of physical methods, the former is easy to perform while the latter has proven to be rather difficult. The adsorption is very easy to perform since it depends solely on Van der Waals forces, ionic interactions and hydrogen binding, while the latter entails a physical confinement of the enzyme on a polymer network. The entrapment requires the use of a hydrogel, and the production of a hydrogel from cellulose has been hindered by the difficulty of dissolving it due to the high crystallinity of the polysaccharide. Both methods have the disadvantage of not having strong bonds between the enzyme and the carrier, making it easy to wash away the enzymes [50]. In

conclusion, adsorption currently seems the easiest and promising alternative, offering the best trade-off between process complexity and yield.

Bibliography

- [1] Iris Beatriz Vega Erramuspe, Elnaz Fazeli, Tuomas Noja, Jani Trygg, Pekka Hinen, Thomas Heinze, and Pedro Fardim. Advanced cellulose fibers for efficient immobilization of enzymes. *Biomacromolecules*, 17(10):3188–3197, 2016.
- [2] Annie Deborah Harris and C Ramalingam. Xylanases and its application in food industry: a review. *Journal of Experimental Sciences*, 1(7), 2010.
- [3] MJ Vazquez, JL Alonso, H Dominguez, and JC Parajo. Xylooligosaccharides: manufacture and applications. *Trends in Food Science & Technology*, 11(11):387–393, 2000.
- [4] Li Fu Chen and George T Tsao. Physical characteristics of porous cellulose beads as supporting material for immobilized enzymes. *Biotechnology and bioengineering*, 18(11):1507–1516, 1976.
- [5] PJ Worsfold. Classification and chemical characteristics of immobilized enzymes (technical report). *Pure and applied chemistry*, 67(4):597–600, 1995.
- [6] Gerald O Aspinnall. *The polysaccharides*. Academic Press, 2014.
- [7] AP Marques, RL Reis, and JA Hunt. The biocompatibility of novel starch-based polymers and composites: in vitro studies. *Biomaterials*, 23(6):1471–1478, 2002.
- [8] Grégorio Crini. Recent developments in polysaccharide-based materials used as adsorbents in wastewater treatment. *Progress in polymer science*, 30(1):38–70, 2005.
- [9] Richard Malcolm Brown and Inder M Saxena. *Cellulose: molecular and structural biology: selected articles on the synthesis, structure, and applications of cellulose*. Springer, 2007.
- [10] Antoinette C O'sullivan. Cellulose: the structure slowly unravels. *Cellulose*, 4(3):173–207, 1997.
- [11] Poonam Singh, Hugo Duarte, Luís Alves, Filipe Antunes, Nicolas Le Moigne, Jan Dormanns, Benoît Duchemin, Mark P Staiger, M Medronho, and M Poletto. From cellulose dissolution and regeneration to added value applications - synergism between molecular understanding and material development. *Cellulose-Fundamental Aspects and Current Trends*, 2015.
- [12] Dieter Klemm, Brigitte Heublein, Hans-Peter Fink, and Andreas Bohn. Cellulose: fascinating biopolymer and sustainable raw material. *Angewandte Chemie International Edition*, 44(22):3358–3393, 2005.

- [13] Sandhi Eko Bramono, Yuen Sean Lam, Say Leong Ong, and Jianzhong He. A mesophilic clostridium species that produces butanol from monosaccharides and hydrogen from polysaccharides. *Bioresource technology*, 102(20):9558–9563, 2011.
- [14] Pastor FI Javier, Gallardo Óscar, Julia Sanz-Aparicio, and Pilar Díaz. Xylanases: molecular properties and applications. In *Industrial enzymes*, pages 65–82. Springer, 2007.
- [15] Regina, Bailey. Cell Wall. <https://www.thoughtco.com/cell-wall-373613>. Online; accessed 20 April 2017.
- [16] Xiaolin Wu, Qinbin Zhang, Zhaokun Wu, Fujun Tai, and Wei Wang. Subcellular locations of potential cell wall proteins in plants: predictors, databases and cross-referencing. *Briefings in Bioinformatics*, 2017.
- [17] Anna Ebringerova and Thomas Heinze. Xylan and xylan derivatives— biopolymers with valuable properties, 1. naturally occurring xylns structures, isolation procedures and properties. *Macromolecular rapid communications*, 21(9):542–556, 2000.
- [18] Annie FA Chimphango, Willem H van Zyl, and Johann F Görgens. Isolation, characterization and enzymatic modification of water soluble xylns from eucalyptus grandis wood and sugarcane bagasse. *Journal of Chemical Technology and Biotechnology*, 87(10):1419–1429, 2012.
- [19] Martin Gericke, Jani Trygg, and Pedro Fardim. Functional cellulose beads: preparation, characterization, and applications. *Chemical reviews*, 113(7):4812–4836, 2013.
- [20] Masayuki Hirota, Naoyuki Tamura, Tsuguyuki Saito, and Akira Isogai. Oxidation of regenerated cellulose with NaClO₂ catalyzed by TEMPO and NaClO under acid-neutral conditions. *Carbohydrate Polymers*, 78(2):330–335, 2009.
- [21] Roger A Sheldon and Sander van Pelt. Enzyme immobilisation in biocatalysis: why, what and how. *Chemical Society Reviews*, 42(15):6223–6235, 2013.
- [22] Jeremy Mark Tymoczko Berg, L John, Lubert Stryer, Jeremy M Berg, John L Tymoczko, Lubert Stryer, et al. *Biochemistry*. 2002.
- [23] KK Wong, LU Tan, and John N Saddler. Multiplicity of beta-1, 4-xylanase in microorganisms: functions and applications. *Microbiological reviews*, 52(3):305, 1988.
- [24] CAZY Carbohydrate Active Enzymes . Glycoside Hydrolase family classification. <http://www.cazy.org/Glycoside-Hydrolases.html>. Online; accessed 25 May 2017.
- [25] Tony Collins, Charles Gerday, and Georges Feller. Xylanases, xylanase families and extremophilic xylanases. *FEMS microbiology reviews*, 29(1):3–23, 2005.
- [26] MLTM Polizeli, ACS Rizzatti, Rubens Monti, HF Terenzi, J AMORIM Jorge, and DS Amorim. Xylanases from fungi: properties and industrial applications. *Applied microbiology and biotechnology*, 67(5):577–591, 2005.

- [27] David L Zechel and Stephen G Withers. Glycosidase mechanisms: anatomy of a finely tuned catalyst. *Accounts of chemical research*, 33(1):11–18, 2000.
- [28] Dietmar Haltrich, Bernd Nidetzky, Klaus D Kulbe, Walter Steiner, and Silvia Župančič. Production of fungal xylanases. *Bioresource Technology*, 58(2):137–161, 1996.
- [29] Linqiu Cao, Luuk van Langen, and Roger A Sheldon. Immobilised enzymes: carrier-bound or carrier-free? *Current opinion in Biotechnology*, 14(4):387–394, 2003.
- [30] E Edet, M Ntekpe, and S Omereji. Current trend in enzyme immobilization: a review. *Int J Mod Biochem*, 2:31–49, 2013.
- [31] Greg T Hermanson. *Bioconjugate techniques*. Academic press, 2013.
- [32] ThermoFischer Scientific. EDC (1-ethyl-3-(3-dimethylaminopropyl)carbodiimide hydrochloride). <https://www.thermofisher.com/order/catalog/product/22980>, . Online; accessed 12 April 2017.
- [33] JULABO. SW22 Banho de água com agitação. <http://www.julabo.com/br/produtos/banho-de-agua-com-agitacao/sw22-banho-de-agua-com-agitacao>. Online; accessed 28 April 2017.
- [34] Poonam Trivedi, Jani Trygg, Tiina Saloranta, and Pedro Fardim. Synthesis of novel zwitterionic cellulose beads by oxidation and coupling chemistry in water. *Cellulose*, 23(3):1751–1761, 2016.
- [35] Mettler Toledo. S470 SevenExcellence pH \ Conductivity. http://www.mt.com/es/en/home/products/Laboratory_Analytics_Browse/pH/benchtop_meter/SevenExcellence/S470.html. Online; accessed 26 April 2017.
- [36] Scandinavian Pulp, Paper and Board SCAN-CM 65:02. Total acidic group content, Conductometric titration method).
- [37] GRANT. Grant Bio PTR60 360° Vertical Multi-Function Rotator. <http://www.grantinstruments.com/ptr-35-and-60-vertical-rotators/gallery/#prettyPhoto>. Online; accessed 28 April 2017.
- [38] HACH. DR 5000™ UV-Vis Spectrophotometer. <https://ca.hach.com/dr-5000-uv-vis-spectrophotometer/product?id=14534087101>. Online; accessed 25 April 2017.
- [39] Eppendorf. Termomixer F1.5. <https://online-shop.eppendorf.com/OC-en/Temperature-Control-and-Mixing-44518/Instruments-44519/Eppendorf-ThermoMixerF-PF-133437.html>, . Online; accessed 25 April 2017.
- [40] Eppendorf. Centrifuge 5810 R. <https://online-shop.eppendorf.com/OC-en/Centrifugation-44533/Centrifuges-44534/Centrifuge-5810--5810R-PF-18809.html>, . Online; accessed 25 April 2017.

- [41] Megazyme. Assay of endo-1-4- β -xylanase activity using AZO-XYLAN (birchwood).
- [42] John Coates. Interpretation of infrared spectra, a practical approach. *Encyclopedia of analytical chemistry*, 2000.
- [43] Francesco Secundo. Conformational changes of enzymes upon immobilisation. *Chemical Society Reviews*, 42(15):6250–6261, 2013.
- [44] Shao-Hua Chiou and Wen-Teng Wu. Immobilization of candida rugosa lipase on chitosan with activation of the hydroxyl groups. *Biomaterials*, 25(2):197–204, 2004.
- [45] Vania CF da Silva, Fabiano J Contesini, and Patrícia de O Carvalho. Characterization and catalytic activity of free and immobilized lipase from aspergillus niger: a comparative study. *Journal of the Brazilian Chemical Society*, 19(8):1468–1474, 2008.
- [46] Christie J Geankoplis, Edwin R Haering, and Michael C Hu. Reaction kinetics and mass-transfer effects in a fixed-bed biochemical reactor with invertase immobilized on alumina. *Industrial & engineering chemistry research*, 26(9):1810–1817, 1987.
- [47] Wilhelm Tischer and Frank Wedekind. Immobilized enzymes: methods and applications. *Biocatalysis-from discovery to application*, pages 95–126, 1999.
- [48] Martin Chaplin. Enzyme Technology - Effects of solute diffusion on the kinetics of immobilised enzymes. <http://www1.lsbu.ac.uk/water/enztech/diffusion.html>. Online; accessed 28 May 2017.
- [49] ThermoFischer Scientific. Sulfo-NHS (N-hydroxysulfosuccinimide). <https://www.thermofisher.com/order/catalog/product/24510>, . Online; accessed 28 April 2017.
- [50] Yue Liu and Jonathan Y Chen. Enzyme immobilization on cellulose matrixes. *Journal of Bioactive and Compatible Polymers*, 31(6):553–567, 2016.
- [51] Youssef Habibi, Lucian A Lucia, and Orlando J Rojas. Cellulose nanocrystals: chemistry, self-assembly, and applications. *Chemical reviews*, 110(6):3479–3500, 2010.

Appendix A

Conductometric titration

The graphs in V-shape of sample 2, 3 and 4 are shown below, as well as zone 2 of each sample.

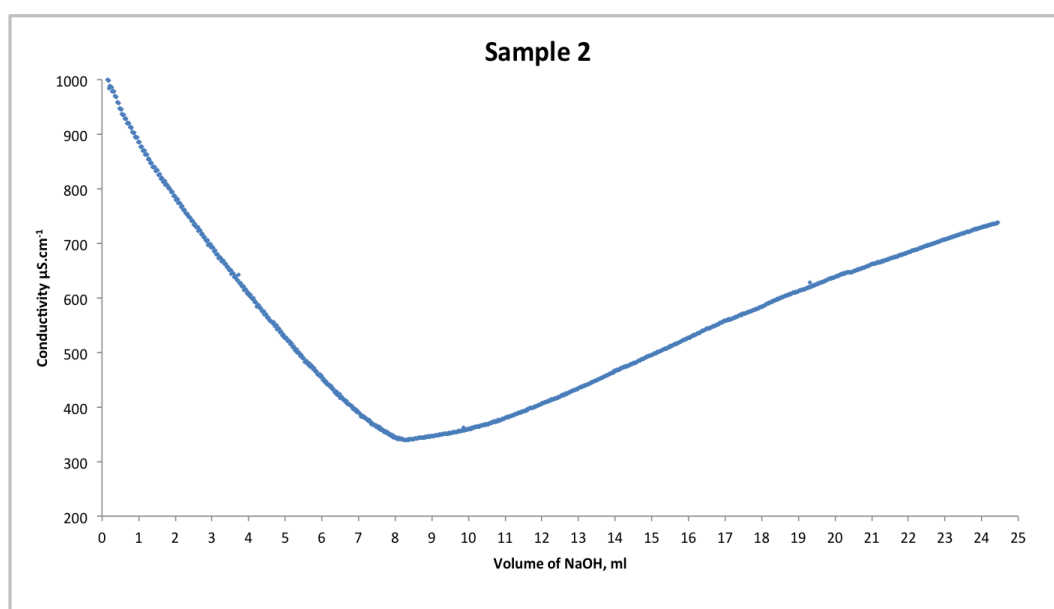


Figure A.1: Conductometric titration graph of sample 2.

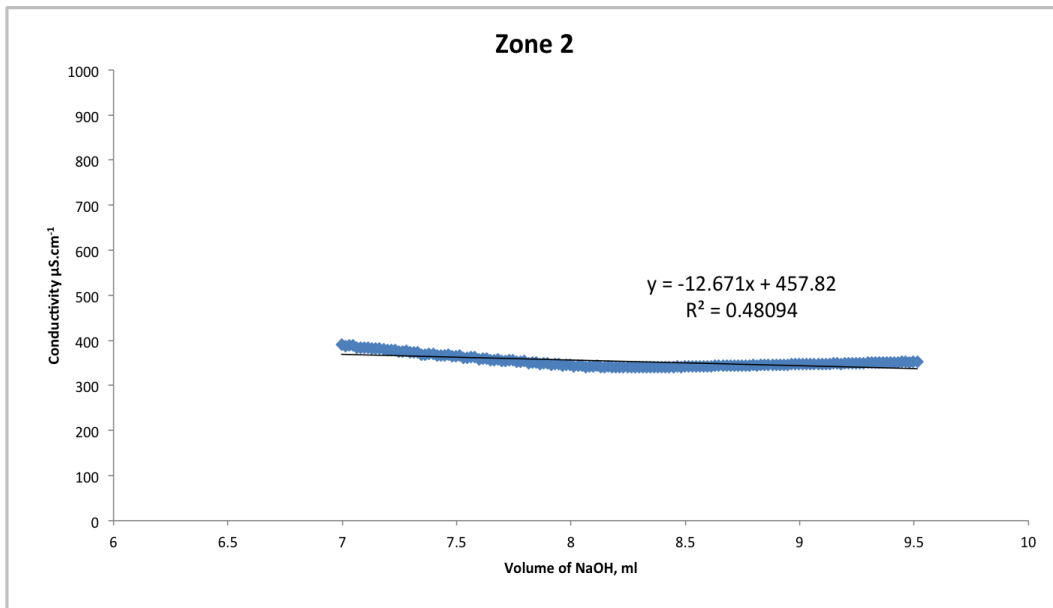


Figure A.2: Zone 2 of the conductometric titration graph of sample 2.

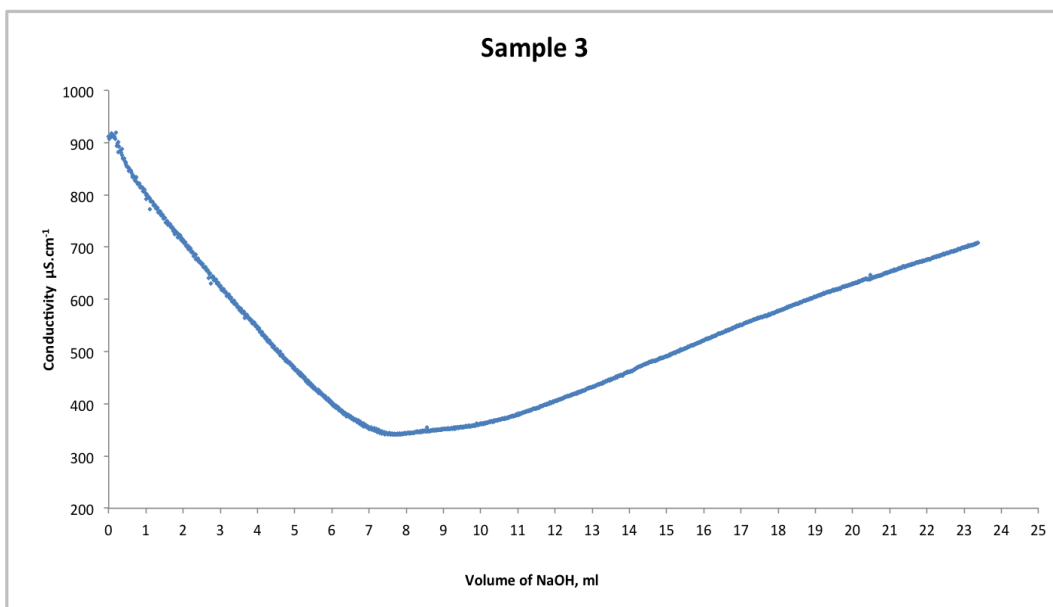


Figure A.3: Conductometric titration graph of sample 3.

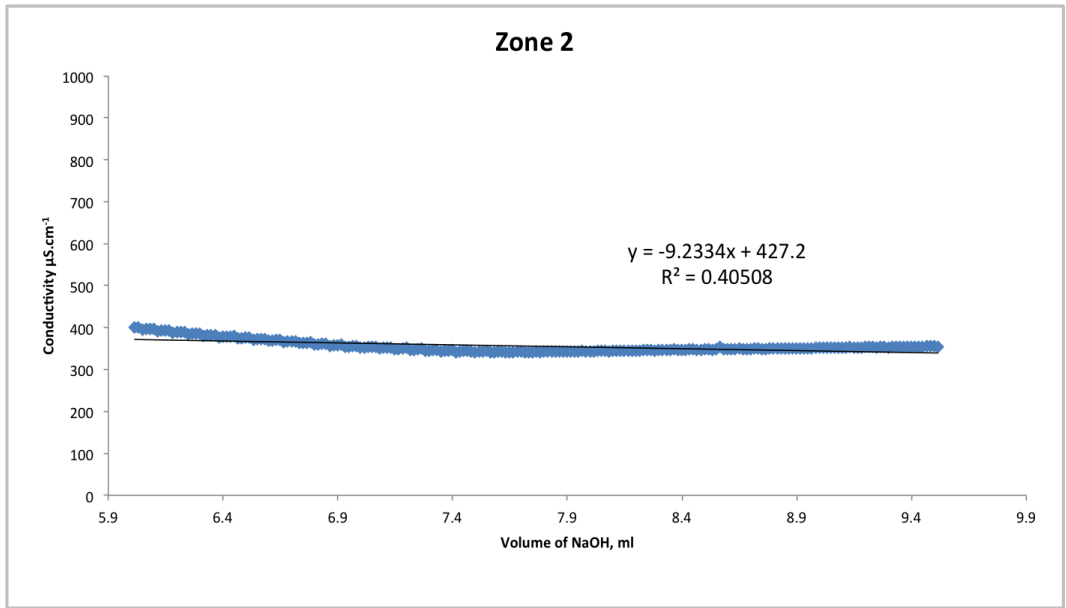


Figure A.4: Zone 2 of the conductometric titration graph of sample 3.

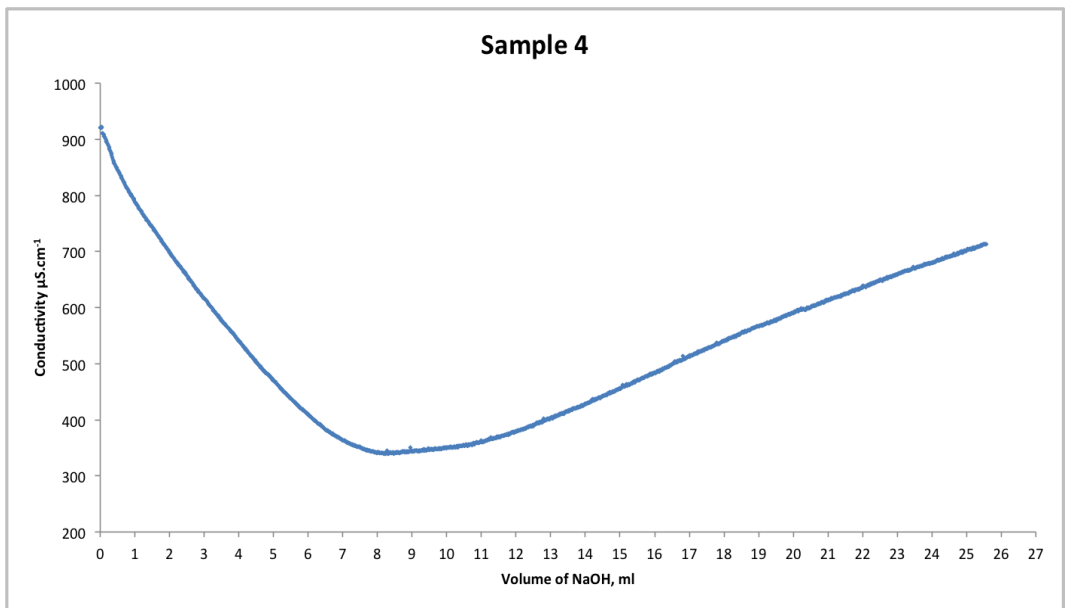


Figure A.5: Conductometric titration graph of sample 4.

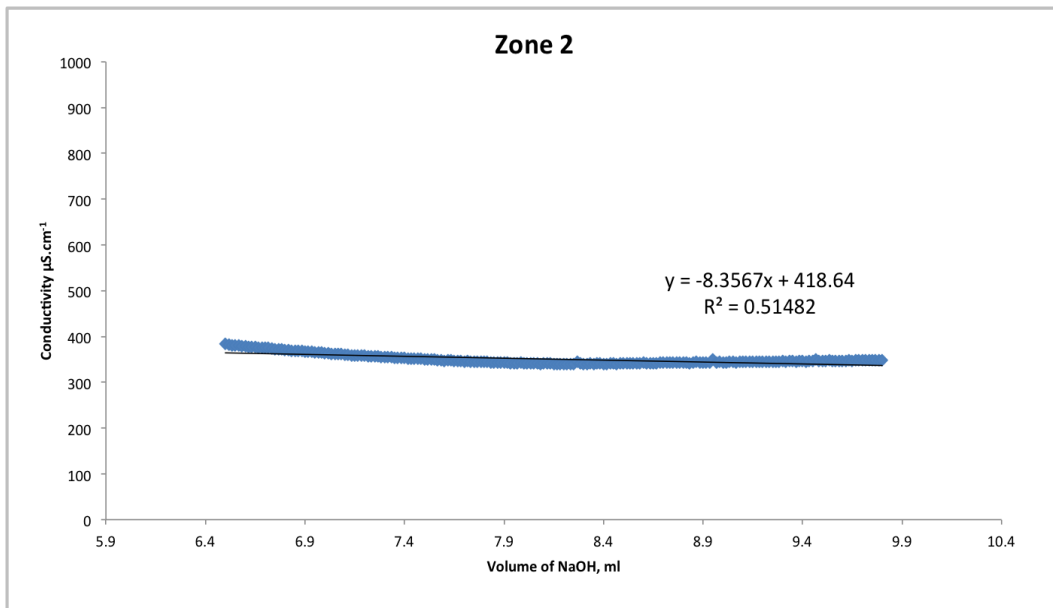


Figure A.6: Zone 2 of the conductometric titration graph of sample 4.

Appendix B

Bradford protein assay

To calculate the concentration (mg.l^{-1}) of xylanase in solution, it is necessary to construct firstly the standard curve. As mentioned in section 3.5 a standard protein such as BSA can be used for this end. It is important to take into account that this technique is extremely sensitive, therefore several dilutions were made until concentrations below 20 mg.l^{-1} were obtained.

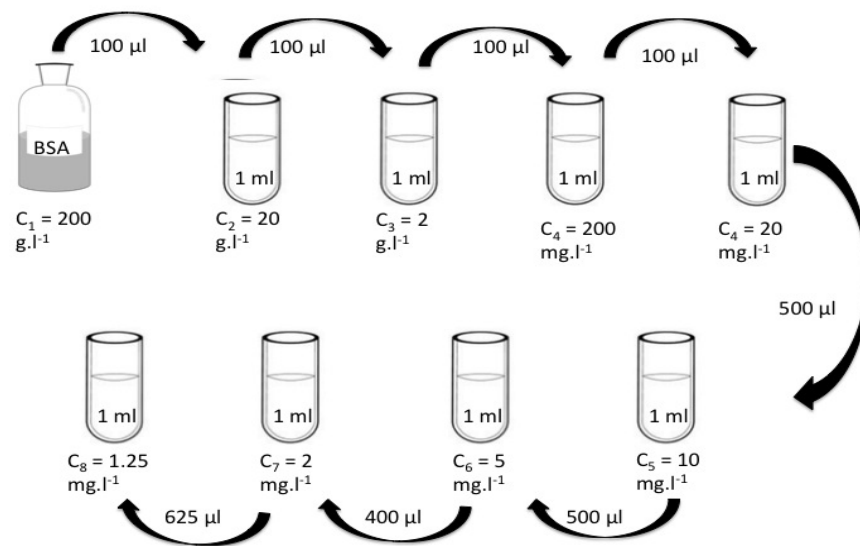


Figure B.1: Scheme of the dilutions made to obtain the standard curve. All dilutions were made with distilled water.

To the last 5 dilutions, $500 \mu\text{l}$ of Bradford were added in order to measure the absorbance of the solution. Table B.1 shows the absorbance obtained for each sample.

Samples concentration (mg.l ⁻¹)	Absorbance
20	0.749
10	0.544
5	0.416
2	0.348
1.25	0.325

Table B.1: Absorbance of the samples tested using the Bradford protein assay.

Using these results, the standard curve was obtained (figure B.2).

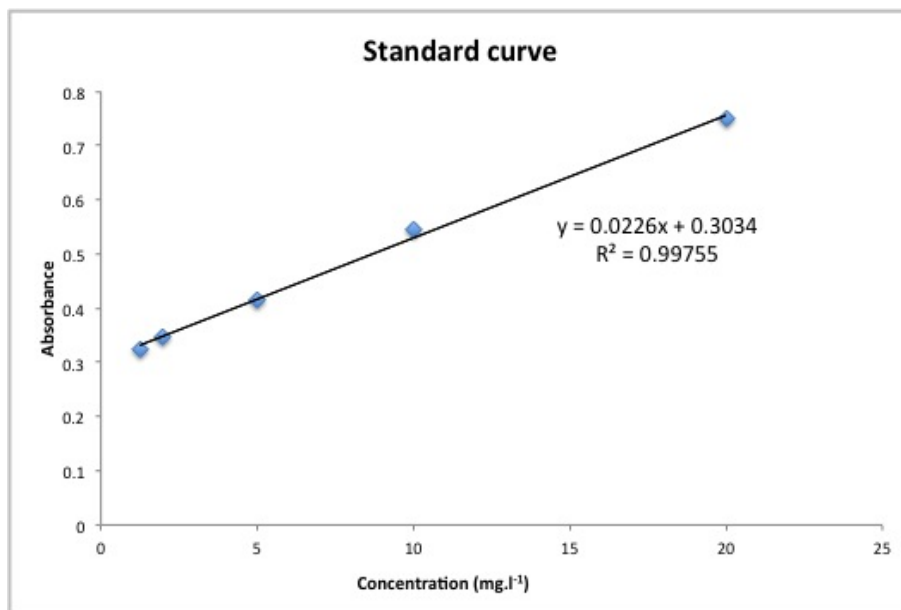


Figure B.2: Standard curve of the Bradford protein assay.